Czech Technical University in Prague

Faculty of Electrical Engineering

Department of Economics, Management and Humanities

Analysis of the effectiveness of the use of positioning systems in solar photovoltaic installations

Master Thesis

Study program: Electrical Engineering, Power Engineering and Management
Field of study: Management of Power Engineering and Electrotechnics
Scientific supervisor: Doc. Ing. Július Bemš, PhD

BSc. Kirillova Daria

Prague 2022

MASTER‘S THESIS ASSIGNMENT

I. Personal and study details

Student's name: **Kirillova Daria** Personal ID number: **511415**

Faculty / Institute: **Faculty of Electrical Engineering**

Department / Institute: **Department of Economics, Management and Humanities**

Study program: **Electrical Engineering, Power Engineering and Management**

Specialisation: **Management of Power Engineering and Electrotechnics**

II. Master’s thesis details

Master’s thesis title in English:

Analysis of the effectiveness of the use of positioning systems in solar photovoltaic installations

Master’s thesis title in Czech:

Analysis of the effectiveness of the use of positioning systems in solar photovoltaic installations

Guidelines:

1. Analysis and review of the necessary technical information about solar trackers;
2. Development of a mathematical model and simulation of installation modes;
3. Calculation of the load of a single-storey house;
4. Evaluate the economic efficiency and feasibility.

Bibliography / sources:

1. Masters GM. Renewable and efficient electric power systems. John Wiley & Sons; 2017.
2. BREALEY, R. A., S. C. MYERS, and F. ALLEN, Principles of Corporate Finance, 10th ed. McGraw-Hill/Irwin, 2010.
3. Yeh PY, Yen PC, Yen JY, Wu TT, Liu PL, Wu CL, et al. Focal point tracking system for concentration solar power collection". Renew Sustain Energy Rev 2011;15:3029–33.

Name and workplace of master’s thesis supervisor:

doc. Ing. Július Bemš, Ph.D. FEE CTU in Prague, K 13116

Name and workplace of second master’s thesis supervisor or consultant:

Date of master’s thesis assignment: **07.02.2022** Deadline for master's thesis submission: **20.05.2022**

Assignment valid until: **30.09.2023**

doc. Ing. Július Bemš, Ph.D. Supervisor’s signature	Head of department’s signature	prof. Mgr. Petr Páta, Ph.D. Dean’s signature

III. Assignment receipt

The student acknowledges that the master’s thesis is an individual work. The student must produce her thesis without the assistance of others, with the exception of provided consultations. Within the master’s thesis, the author must state the names of consultants and include a list of references.

.	
Date of assignment receipt	Student’s signature

Declaration

I hereby declare that this master's thesis is the product of my own independent work and that I have clearly stated all information sources used in the thesis according to Methodological Instruction No. 1/2009 – "On maintaining ethical principles when working on a university final project, CTU in Prague".

Date *Signature*

Abstract

Currently, there is a need to create an efficient and inexpensive installation that could use alternative energy sources to produce electricity. One of the promising areas of renewable energy - solar energy. To convert the energy of the sun into electrical energy a special device is needed - a solar panel, as well as a number of other, auxiliary devices. In this paper, we propose a way to increase the productivity of solar panels through the use of sun-tracking installation - a solar tracker.

The result of this dissertation is a finished model of the solar plant with an integrated model of the solar tracker, created in the Matlab/Simulink software product. With its help, the potential of the area was assessed (three geographical points were selected - Alexandrovskoe village, Brno and Shanghai), and the possible power generation of the considered installation with and without the use of different types of tracker was determined.

The thesis is structured as follows: first I describe a review and analysis of the use of solar trackers in world practice. Then the development of a mathematical model of the tracking system. Then the simulation of the tracking system operation modes is presented. In the next chapter, I built a power supply system using solar trackers. Then the economic evaluation of the investment solution was carried out.

The conclusion will be made about the technical and economic efficiency of the use of solar trackers, a comparative analysis of the performance of different models.

Contents

List of Abbreviations

ST	Solar tracker
PVS	Photo-Voltaic Station
HSAT	Horizontal single-axis tracker
HTSAT	Horizontal with tilted modules single-axis tracker
VSAT	Vertical single-axis tracker
TSAT	Tilted single-axis tracker
PSAT	Polar single-axis tracker
AC	Alternative current
DC	Direct current

Introduction

In today's world, the greatest interest is the use of sunlight energy [5]. This type of application is called photovoltaics (Photovoltaic, abbreviated PV). The end product is photovoltaics.

There are several ways to increase the performance of photovoltaic plants. The first is to choose a substance with a higher photovoltaic power. At this stage of science, such substances are gallium arsenide, germanium, chalcogenides, and others. The photovoltaic conversion coefficient with these substances increases up to 32% [7].

The second method is maximum power point tracking (MPPT). Implementation of the method involves the use of microprocessor technology, controllers. In most modern solar inverters you can find such a system. The essence of the method is the following: the controller analyses the volt-ampere characteristic (VAM) of the battery and looks for the optimal mode of operation, which will ensure the production of the maximum amount of energy at a given illumination.

The third way is to track the position of the Sun in the sky. The solar tracker discussed in this article is designed to solve this problem.

A sun tracker is a sun tracking system that allows you to track the trajectory of the Sun according to pre-defined algorithms, and based on this, change the position of the receiving surface of the solar cell. Most trackers are divided into single-axis and two-axis trackers. Single-axis trackers change the position of the solar cell only in one plane, and biaxial trackers can rotate it in two planes at once.

Experience in the operation of solar position tracking systems in different countries shows that their use increases the performance of the photovoltaic system from 15 to 72%, depending on the type of tracker, the geographical location of the power plant, climatic conditions, and time of year [8]. According to GTM Research's Global PV Tracker Landscape 2016 report, 12.6 GW of PVS installations with solar trackers are installed worldwide this year, and by 2021 the number of tracker installations will grow to 37.7 GW, which will be almost half of all ground-mounted solar installations. According to Zion Research, the global solar photovoltaic tracker market is expected to reach $3,682.2 million in 2021. The market is expected to reach $3,682.2 million from 2016 to 2021, growing at 18.6% per year. [9]

Currently, however, the least studied way to increase the efficiency of converting sunlight energy into electricity remains the use of trackers. This is because the information on methods of calculation and creation of mathematical models of solar tracker components is scattered, little ordered. However, the method under consideration is the most suitable for an application, since it does not require expensive study of the properties of already existing and obtaining new semiconductor materials. Therefore, the goal of this work is to develop an optimal mathematical model of the tracker, which would provide the maximum performance of the solar panel, great accuracy in tracking the position of the Sun in the sky, ease of installation, and cost-effectiveness.

1. Review and analysis of the use of solar trackers in world practice

There is already a high and constantly growing demand for electricity [10, 11]. In this regard, the generation of energy from solar radiation has excellent prospects in the renewable energy industry. Conversion of solar radiation into electricity is carried out both by photovoltaic panels and solar energy concentration systems. The output power of these devices depends on the amount of solar radiation they can receive [12].

Various devices and adaptations have been developed to improve the energy performance of photovoltaic panels. One such device is the solar tracker. It is designed to orient the solar panel surface to the Sun and track it. Finster [13] introduced the first solar tracker in 1962. This system was reportedly mechanical and much less productive than stationary units. A year later, Saavedra [14] presented an improved version with an automatic electronic control unit and a pyrheliometer to measure the amount of direct solar radiation on a surface perpendicular to the sun's rays. In 1975, McPhee [15] proposed another type of ST with a different algorithm, which was capable of calculating the total received solar radiation and flux density distribution over the entire system of solar installations [15,16]. Additional mirrors were installed in the system, and the position of the sun was calculated by summing the amount of solar radiation received by each installation. The tracking error of this system was about 0.5° to 1°. A few years later, Semma and Imammura [17] used a microprocessor to adaptively adjust the position of the solar collectors of a thermal photovoltaic concentrator. Several more studies followed, and additional mathematical models were developed to improve the then-existing algorithms [18-21]. Significant improvements in the accuracy of the ST has been seen since 1985, following the work of Badescu [22], in which he demonstrated the influence of astronomical and design parameters on the concentration of solar radiation on the surfaces of photovoltaic systems equipped with tracking systems.

Commercialization of solar trackers began in early 1980 after the work of Dorian and Nelson [23], who developed an automatic solar tracking system capable of directing a solar collector to the Sun throughout the day. This system found application in real life, but it still had low efficiency and required upgrades. In 1983, Maldonado [14] proposed a servo-controlled algorithm for tracking the Sun, which made it possible to automatically orient the pyrheliometer to the Sun and calculate the position of the Sun using a computer program. A later study by the authors [24] proposed a new generation of trackers with microprocessors and electro-optical controllers.

In recent years, the latest technologies have been developed to increase the amount of solar energy generated by these systems using direct and indirect methods. Some of these methods include, but are not limited to the use of solar trackers and the selection of the optimal angle of the installation, which allows them to collect the greatest amount of available solar radiation [4, 5]. However, there are still some limitations in these methods [6], which can be overcome only by the application of ST, provided the optimal parameters of the installation and control system [7]. Ideal trackers can orient photovoltaic panels to the Sun with high accuracy, and, in addition, compensate for daily changes in the sun's elevation angle and seasonal latitude shift, as well as changes in the azimuthal angle.

The slow motion of the sun requires reliable and stable operation of the tracker control system, which must track this motion. When designing a solar tracker system, the focus should be on the configuration of the rotation axes [8, 9], the improvement of their moving attachments [10], and the proper tuning of the control systems [11]. Each of these components has its features, advantages, and disadvantages [8], which can be easily manipulated to increase the total amount of energy collected by the tracker.

STs allow to accurately orient photovoltaic panels to the sun and to cover losses during the change of time of day and time of year, observed in the angles of sunrise height, azimuth, and latitude. Consistent with the above, studies [34] have proven that the amount of solar energy generated by any tracker photovoltaic panel is always greater than that obtained from a simple stationary panel. For this reason, several methods [26, 35] have been investigated to establish the feasibility of these systems. In most cases, a tracker consists of the following parts:

- A frame and rack;
- One or two motors;
- Light sensors powered by independent or auxiliary power supplies;
- A dynamic and stepper motion controller;
- positioning adjustment mechanism [36].

The use of sun-tracking devices and systems is a promising area of study. Currently, there is a demand for such systems, which would allow to orient the receiver site perpendicular to the sun's rays to achieve maximum performance of the generating photovoltaic installation. One such system is solar trackers, which have their classification.

1.1 Parameters of solar radiation

The term "solar radiation" falls under the corpuscular-wave theory, that is, it is an electromagnetic wave and a stream of particles simultaneously. Accordingly, it has a certain reserve of energy, which is carried from the Sun. According to [53], solar radiation is formed from several components:

• S_{nakl} - direct solar radiation,

• D_{nakl} - scattered solar radiation,

• R_{nakl} - reflected solar radiation.

In addition, there is such a parameter as - solar constant, which characterizes the energy of solar radiation outside the Earth's atmosphere.

Figure 1.1 shows a diagram, which gives an idea of the geometric dependencies in the calculation of solar radiation.

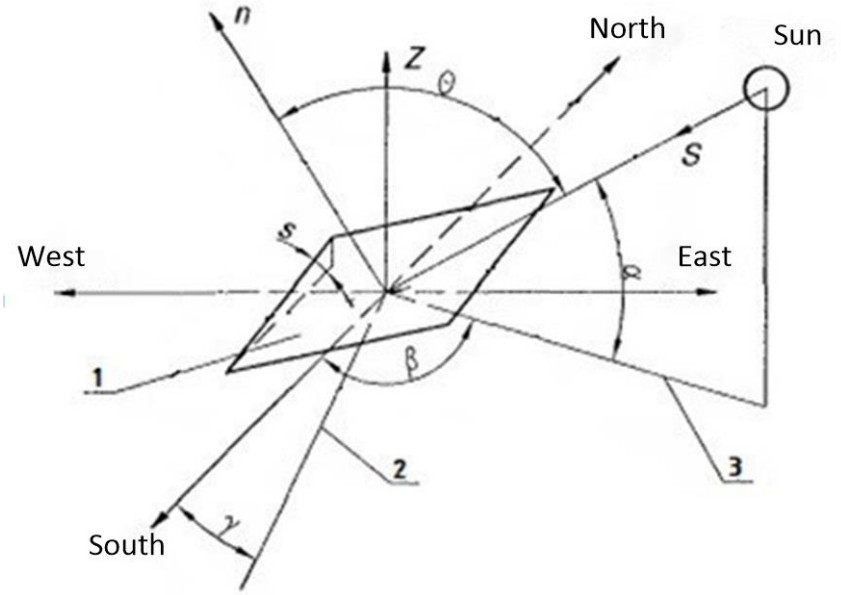

Figure 1.1 - Schematic for calculating solar radiation on an arbitrarily oriented surface:1 - arbitrarily oriented surface, 2 - horizontal projection of the normal, 3 - horizontal projection of the solar ray, Z - normal to the horizontal plane, n - normal to the inclined plane, S - direct solar radiation on the Earth surface, α - elevation angle of the Sun, β - the azimuthal angle of the Sun, γ - the azimuthal angle of surface 1, θ - incidence angle of direct solar ray on plane 1, s - inclination angle of plane 1.

To convert the received solar energy, there are solar power plants, or photovoltaic installations (stations).

1.2 Photovoltaic installations

Photovoltaic installation (station) is a set of devices that convert the energy of solar radiation into electrical energy. As a rule, PVS consists of solar panels, storage batteries, battery charge controllers, and inverters. Figure 1.2 shows an approximate composition of PVS.

Figure 1.2 - Composition of the PVS: 1 - Solar battery, 2 - battery charge controller and inverter in one case, 3 – battery

Thus, it is obvious that to increase the energy generated by the PVS, a solar tracker can be introduced into its composition.

1.3 Classification of trackers

The classification of these devices depends on many different parameters, including the operating model and control force. Each of these systems presents its advantages and disadvantages. Particular attention should be paid to price, reliability, power consumption, and maintenance.

Currently, solar trackers are conventionally divided into two main groups: single-axis trackers (rotate the panel around one axis) [12-16] and dual-axis trackers (rotate the panel around two axes) [17-20]. However, other studies [21, 22] highlight other types of trackers with much more complex structures, but they are not as much in demand. There is also a classification according to the type of rotation mechanism: passive and active.

Passive solar trackers do not use mechanical actuators in their work to orient the perceiving surfaces to the direction of solar radiation. They have less complex structures and have no limitations or disadvantages in hardware implementation [37]. The principle of their functioning is quite simple: most of them have a pair of actuators filled with an expandable gas [38] or an alloy with a shape memory effect [38]. These actuators work in opposition to each other and are in a state of equilibrium under uniform illumination. The latter causes thermal expansion of the gases or alloy. Any change in module illumination throws the actuator system out of equilibrium, hence the orientation of the panel until equilibrium is restored again. Figure 1.3 shows a simple passive tracker with two identical cylindrical tubes filled with an expanding liquid.

As the liquefied gas is heated on one side (due to uneven illumination), it expands and spreads to the opposite side of the tracker, causing the PV panel to tilt toward the sun before reaching the point of equal illumination [39]. Such passive STs, in which liquefied gas is used, are more advantageous, because they have no parasitic force on the frame rotation axes when moving.

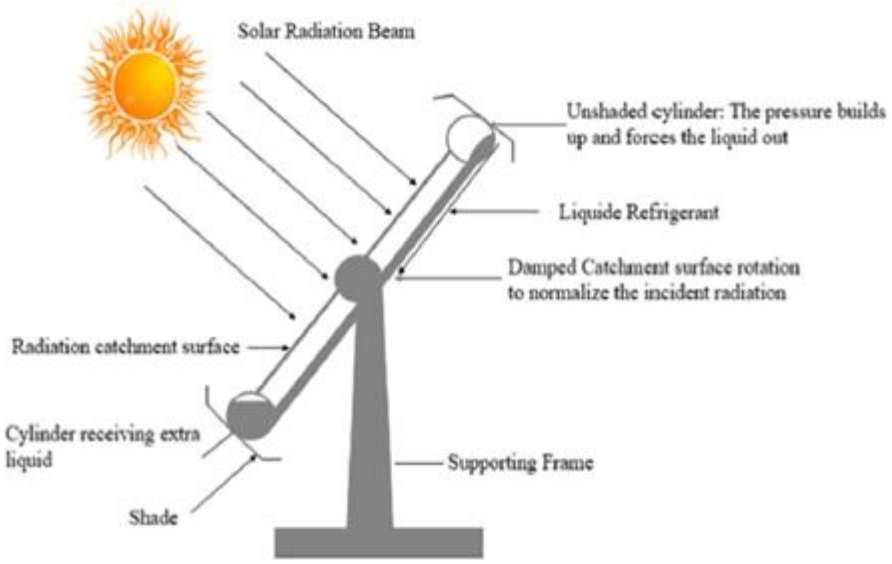

Figure 1.3 - Passive ST with two identical cylindrical tubes with a working fluid under partial pressure [38]

The liquefied gas creates a slight change in the weight of the installation, just enough to shift the panel to its most optimal position. The firmly welded frames do not deform and do not change their position even when the panel is exposed to strong gusts of wind, making them reliable. Moreover, their parts show high resistance to wear and tear. Consequently, they do not require high maintenance costs. Nevertheless, such systems require seasonal axle adjustments, as well as annual painting and bearing lubrication [34].

In 1998, Lorenz [35] proposed a set of parameters used in the design of glazing that reflected solar radiation in summer and absorbed it in winter. The system had a purely passive control algorithm based on seasonal changes in the angle of incidence of solar radiation. A few years later, Clifford and Eastwood [38] proposed an inexpensive model of a passive solar tracker mounted on a wooden frame, symmetrically on either side of the central horizontal axis. The movements of the system were controlled by both aluminum or steel bimetallic plates and a friction damper (to prevent oscillations or passive triggers). Simulation results and real-time measurements showed a 23% increase in energy compared to a stationary solar panel. Importantly, the bimetallic plates created enough force to move the panel even with small solar movements, making them more cost-effective.

Similarly, the author [37] proposed a single-axis passive tracker driven by actuators filled with an alloy with a shape memory effect. It was used to increase the efficiency of a solar dryer for coffee beans. The actuator acted as a heat engine and could function even when exposed to temperatures of 70°C (the alloy would return to its original shape). The initial angle of 60° was set to the east every morning (8:00 am) to the horizon. Observations showed that the solar dryer successfully reduced the drying time of the grain by 5-7 days (solar drying). In addition, the temperature inside the chamber reached a maximum of 70.4 °C.

Passive STs are easy to use and consist of less complicated structures. Moreover, they do not require any additional power supply because they work directly with solar radiation. However, they give a lower energy gain than their active counterparts. Another serious problem is that they cannot be used in regions with extremely cold weather conditions, as they instantly stop working at low temperatures. Although they are cheaper and require less additional equipment to install, they are not yet widespread enough, making their use limited.

Active STs are also called continuous trackers and use both sensors and electric motors in their operation. The sensors (mostly 2) help them continuously determine the position of the sun in the sky, and the electric motors help them orient the panel to it. Their general design and control algorithms are shown in Figures 1.4 and 1.5.

The active ST has a pair of sensors that send a compound signal that causes motors or actuators to move, which in turn move the photovoltaic panel behind the sun. When the solar flux and the solar panel are not on the same normal, these sensors receive different amounts of light, creating different signals that are used to determine the direction in which the tracker should move (see Figure 1.4). The tracker stops moving when both sensors are equally illuminated i.e., the solar flux is perpendicular to the photopanel. Literature [34] indicates that this method of tracking the sun is quite accurate, except on very cloudy days when it becomes quite difficult for the sensors to accurately determine the relative position of the sun.

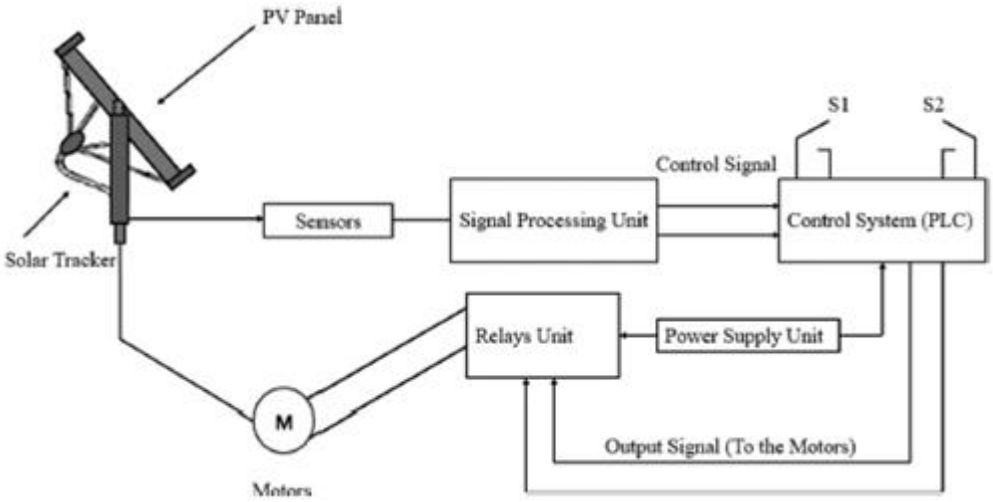

Figure 1.4 - Block diagram of the active solar tracker [34]

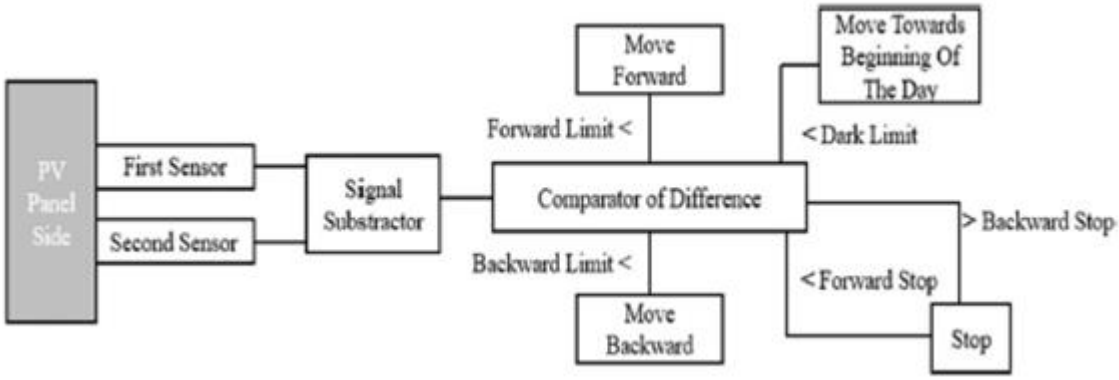

Figure 1.5 - The logical sequence of the control process of the active solar tracker [34]

Active solar trackers are usually classified into trackers with microprocessor and electro-optical sensors, computer-controlled by date and time, trackers possessing an auxiliary two-way solar array, and combined trackers. All electro-optical STs in general have at least one pair of antiparallel photosensors/photopanels that are electrically balanced (equal amount of light of both units). In auxiliary solar cells, a double-sided photocell captures the sunlight and orients the system to the desired position. In the trackers, controlled by the computer by date and time, an algorithm is written to analyze the date and time of the terrain, by which the position of the sun is determined and control signals are generated.

Single-axis STs have a single axis of rotation, which can be oriented in almost any direction if advanced control systems are used. However, studies [34] show that while orientation along the north meridian axis is the preferred orientation, module orientation relative to the tracker axis is important when modeling possible performance. There are several configurations of single-axis trackers, including horizontal (HSAT), horizontal with tilted modules (HTSAT), vertical (VSAT), tilted (TSAT) and polar axis oriented (PSAT). A special case of VSATs is the azimuthal angle tracker, which specifies the azimuthal angle of the Sun's position for the reception site. In turn, a special case of HSAT tracker is the tracker on the angle of ascent of the Sun. It orients the surface of the receiving pad, depending on the angle by which

the Sun rose above the horizon. The authors [40] conducted an extensive study of all these systems and concluded that VSATs are more efficient among all single-axis trackers. Their research drew a number of conclusions about how single-axis STs should be designed and tuned in order to maximize the collection of solar radiation.

The study in [41] showed that HSATs are very flexible and equally capable of keeping all their axes of rotation parallel to each other throughout the tracking time. The study in [40] confirmed that the HTSATs work like the HSATs with the only difference being that the HTSATs are mounted at a certain tilt. They are usually suitable at high latitudes and save space compared to other types of single-axis trackers due to their orientation. A typical HTSAT is shown in Figure 1.4 [42].

VSAT trackers track the Sun on the vertical axis [12] and are more effective at high latitudes than horizontal trackers, but need more space to avoid shading and obstruction from other trackers nearby [42]. A typical diagram is shown in Figure 1.6 below.

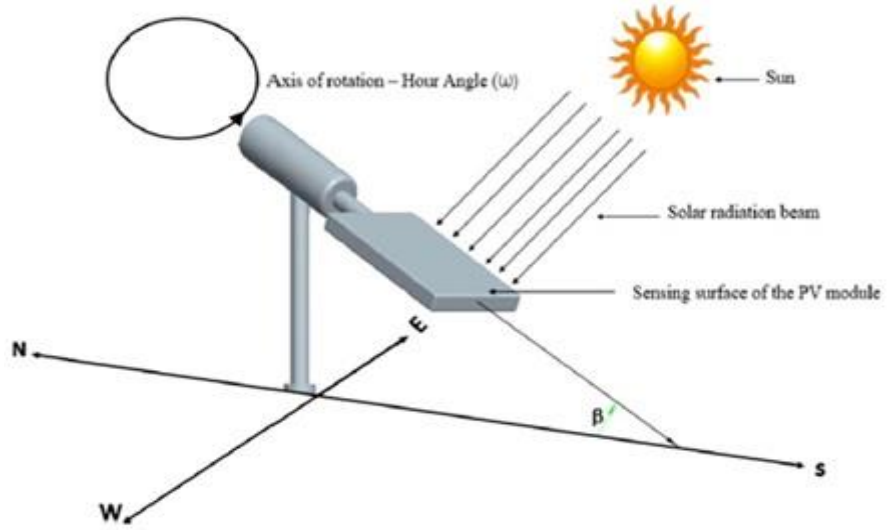

Figure 1.6 - Horizontal single-axis tracker with tilt module [41]

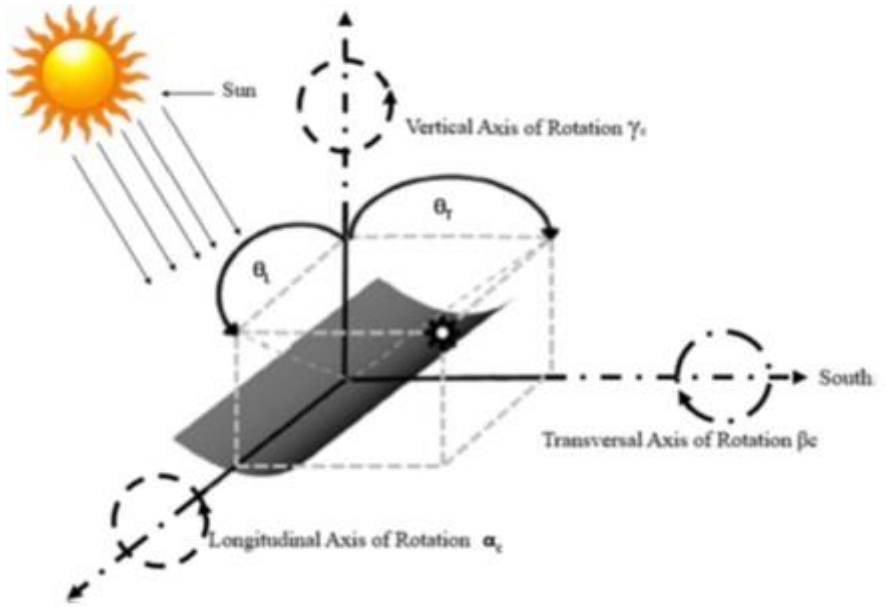

Figure 1.7 - VSAT angles: tracking angle, manifold tilt, manifold azimuth, longitudinal angle, and transverse angles [12]

TSAT have an axis of rotation located between the horizontal and vertical axes, giving them a strong resistance to the effects of strong winds and shading from other trackers. They can easily be set to reverse tracking if their tilt and latitude angles are properly selected. PASAT trackers are installed according to standard telescope installation methods. Some researchers [12, 14-16, 43] suggest that their tilt angle should be equal to their latitude so that both axes of rotation can be perfectly aligned. Most of the aforementioned studies on these types of trackers show 5% to 25% power gains over stationary systems [15, 30]. Let's add that the above mentioned efficiency can increase up to 30% in regions with more solar resources [44] and question the cost of biaxial solar trackers [36].

Thus, I can distinguish two types of solar trackers: single-axis and double-axis. Their use gives an increase in the capacity of the generating photovoltaic plant when using a single-axis system from 5 to 30%, depending on the geographical location, weather conditions, and other factors. Using a two-axis tracker provides an additional gain of 5-7% over a single-axis tracker, which makes its use not economically justified.

1.4 World experience in the use of solar trackers

Literature shows that solar trackers are fairly used all over the world because of their simple design and the simplicity of implementation of their control systems. Following the above, the authors [45] proposed a simple single-axis ST, characterized by a new arrangement of auxiliary bilateral solar panels, which are directly connected to the DC motor that drives them. In a similar study, the author [46] proposed a single-pole tracker with a solar collector to track the sun within 15°/h. Researchers [47] proposed a new single-axis azimuthal tracker that moves the solar collector tracking surface in two directions through special support fixtures. The author [48] investigated an active uniaxial solar tracker used for planar PV systems and achieved 20% more efficiency compared to stationary PV panels. The author [49] presented a PV panel fixed on a single-axis tracker and achieved a 17.5% increase in energy compared to stationary systems.

Extensive research has been done in recent years [21, 25-27, 50] to improve the efficiency and stimulate the use of dual-axis STs. Although single-axis trackers are much cheaper and easier to build, their efficiency is lower than that of biaxial trackers. In addition, studies [25] have shown that some solar system objects require two-axis trackers because of their advantages, such as the ability to absorb maximum solar radiation and then produce the maximum amount of energy.

According to the aforementioned authors, the researchers [50] confirmed that the biaxial ST always generated more power output compared to the single-axis and stationary PV panels. A study [51] compared the output parameters of stationary PV panels and biaxial STs and found that the biaxial tracker achieved an energy increase of 34.6%. A similar study was conducted in [52] with the biaxial ST showing energy increases of 128 W (30%) and 413 W (44%) in winter and summer, respectively. The data are presented in comparison with the single-axis tracker. A recent study by the authors [53] proposed a highly accurate two-axis solar tracker using an algorithm with image processing capabilities to estimate system pointing errors reaching an accuracy of ± 0.1°. In 2012, a group of scientists [54] developed a high-precision tracking

system that achieved a 0.01% standard deviation between simulated and measured values of available solar radiation. Many other researchers [12, 13, 17, 18, 39, 55, 56, 57-59] have focused on two-axis trackers and developed advanced algorithms. The overall conclusion from all this work is that biaxial STs have always achieved good results with 20% and 50% higher energy efficiency compared to stationary PV panels.

Recent advances in solar panel production, advanced computer technology, and modern electronic control systems provide additional opportunities for research to optimize the design and mode algorithms of ST operation. Significant progress is now being made in improving efficiency [7, 23-25] in clear and cloudy weather [8, 26].

The production of tracking systems and the photo panels themselves is becoming more environmentally friendly [27-30]. Because of this, STs provide up to a 100% increase in energy storage compared to fixed photovoltaic panels of the same size, optimally directed toward the sun [26, 31-33] depending on the season, time of year, and location [34]. Studies [34] show that a great deal of work has previously been done with various solar position tracking algorithms in an attempt to improve their efficiency and obtain more optimized systems.

In most cases, single-axis trackers can effortlessly increase the generated energy by 12-20% compared to stationary systems [23]. It is also possible to achieve an increase in energy production of up to 30% by selecting the most optimal tracker parameters [18, 32]. Moreover, while many researchers refrain from using single-axis trackers, Huang and Song [36] have demonstrated their achievements. They were able to increase energy generation by 56% by implementing special designs and control systems. In the case of two-axis trackers, an annual energy gain of 20.4% was achieved in [37] and 43.9% in a similar study [38] compared to optimally oriented panels. Senpinar and Jebeji [39] achieved an energy increase of 13.25% more than stationary systems of the same size delivered. Several other researchers have compared the efficiency of single-axis and dual-axis trackers and found the former to be 3-5% inferior to the latter [9]. It follows from the above that CTs are a versatile tool, suitable for solving specific problems of increasing the amount of collected energy [34, 40].

Authors in the literature [30, 35, 31] argue that two-axis trackers are more efficient and also more cost-effective for applications in large photovoltaic systems. Other studies [8, 26, 39] show that the performance of two-axis trackers can be complicated by unfavorable environmental conditions. Among some researchers, there is a perception that STs may become obsolete due to their complexity and operating costs [42, 43]; a study [26] shows that these technologies are ubiquitous throughout the world, and there is a large amount of research underway to address the problems and limitations associated with their technical design and cost-effectiveness of solar trackers. According to the aforementioned authors, Huang et al. [43] confirmed that there is no doubt that dual-axis trackers produce more electricity than single-axis trackers. However, they also argue that their solution is justified only if the amount of electrical energy produced compensates for the equipment costs, the energy consumed by the moving parts, and the installation and operation costs. It follows that when optimizing the parameters of trackers, attention should be paid to removing the above-mentioned limitations, disadvantages, and problems.

Current literature has made the necessary recommendations and descriptions to reduce the prices, the tracking systems considered, and to achieve the best level of solar energy collection. Regarding the technical issues, Huang and Son [33] think that photovoltaic modules should be connected either in series or in parallel on the same tracker and that the equipment used should be chosen optimally to save costs. The authors [31] recommend using a method of simultaneous control of a section of PV modules, which will reduce the price and limit the energy cost of control to more than 20%. Their method involves the simultaneous transfer of motion to all section modules through a polygonal mechanism, which is driven by a single motor. For economic reasons, the researchers in [32] suggest using the same, large photovoltaic systems for both large and small solar panels. Moreover, since the temperature is one of the parameters that affect the performance of PV systems [26, 44-47] when making panels for installation in deserts or other high-temperature regions, priority should be given to materials with higher thermal resistance. Exposure of silicon panels to high temperature reduces their efficiency [48] by 0.5% for each degree Celsius increase in temperature [49].

The trackers are designed to track the movement of the sun along one or more axes. This keeps the surface of the photovoltaic panel perpendicular to the direction of solar radiation. There are also other requirements for the ST: night movement of the tracker to anticipate sunrise, compensation for temporal and seasonal variations observed in the sun's elevation above the Earth's surface, latitude, and azimuthal angles of the sun. The main goal pursued by all developers is to increase the amount of solar radiation the system receives. Studies [28] show that two-axis trackers are more accurate and affordable compared to their single- and multi-axis counterparts. Their performance is always at least 98.5% efficient even when the tracking accuracy is 10°. Although this tracking error is acceptable and causes significant energy loss, it must nevertheless be minimized to ensure maximum plant efficiency. Typically, under favorable conditions, the total annual energy gain from using a dual-axis tracker ranges from 30% to 40%. However, in foggy and snowy terrain, it can even reach less than 20% of its maximum capability.

1.5 Goals and objectives of the work

Thus some problems arise: what type of tracker should be installed in this or that area, whether it makes sense to install this device at all, what algorithm of operation to choose.

To answer these questions, the following problems must be solved:

1. Develop a mathematical model of the process of solar radiation arrival, as well as a model of the photovoltaic installation;
2. To test the adequacy of the model on specific geographical objects located in different parts of the country;
3. Use modeling to test the development to determine the most effective type of tracker for a particular location in the world;
4. Evaluate the cost-effectiveness of the project by comparing similar indicators in the application of different types of trackers.

To solve the above-mentioned tasks, the mathematical modeling environment Matlab/Simulink is used. In this work, the methods of model-oriented mathematical research, simulation modeling, algorithmization are applied.

The relevance of the work is confirmed by the growing interest in the use of alternative sources, mostly solar energy, for power supply of remote, isolated, hard-to-reach, and economically inexpedient for electrification areas of both Russia and the world. In addition, another no less urgent question of optimizing the parameters of photovoltaic installations by introducing a solar tracker into them is touched upon.

The scientific and practical value of the work lies in the development of software that allows not only stimulates the process of solar radiation on the PV panel and transforms it into electrical energy but also allows optimizing and improving the performance of photovoltaic installations by 30% (meaning that the application of the tracker gives an increase in the output of up to 30% depending on locality, that is without a tracker there will be some pure, and with a tracker, there will be + 30%).

1.6 The final result of chapter 1

There are many models of solar trackers in the world. They are divided into single-axis and double-axis. Over time, this technology has evolved and expanded with all sorts of additional devices: motors, controllers, etc.

In the reviewed models, among other things, there is a certain algorithm, based on which the tracking of the Sun takes place. The algorithm may be based on the principle of maximum power search, rotation of photopanels at certain times during the day, etc. However, the most reliable and accurate way is orientation by solar position.

In addition, it makes sense to use a different type of tracker at different geographical points of the planet. In countries where there is more solar radiation and, accordingly, more light days and the duration of the daylight itself, it makes sense to install a two-axis tracker. Where solar radiation is scarce, but there is a question of increasing the performance of the system, the best option would be to install a single-axis solar tracker.

2. Development of a mathematical model of the tracking system

2.1 Model of the arrival of solar radiation on the surface of the solar panel

Mathematical modeling of solar tracking systems has been considered in [50-52]. According to [53], solar radiation on an arbitrary-oriented receiving surface consists of three solar radiation streams: direct solar radiation falling on the inclined surface S_{tilt}, scattered radiation falling on the inclined surface D_{tilt}, and radiation reflected from the Earth's surface R_{tilt}. The magnitude of radiation depends on many factors: mutual location of the receiving surface and the Sun, change of this location over time, location of the receiving surface relative to the ground, as well as a level of cloudiness and transparency of the atmosphere. The value of solar radiation hitting an arbitrarily oriented receiving site on the Earth's surface is calculated according to the formula:

$$Q_{\text{tilt}} = S_{\text{tilt}} + D_{\text{tilt}} + R_{\text{tilt}} \quad (0.1)$$

The importance of direct solar radiation S_{tilt}:

$$S_{\text{tilt}} = S_{ort} \cos\theta, \tag{0.2}$$

where S_{ort} – direct solar radiation on a plane orthogonal to the rays, (W/m^2);

θ –angle between the direction of solar radiation flux to the receiving surface and the normal to it, (rad).

Kastrov's formula defines S_{ort}:

$$S_{ort} = \frac{S_0 \sin\alpha}{\sin\alpha + c}, \tag{0.3}$$

where S_0 – solar constant, W/m^2;

c – value characterizing the degree of atmospheric transparency.

Angle value θ is defined from the expression:

$$\cos\theta = (A - B)\sin\delta + [C\sin\omega + (D + E)\cos\omega]\cos\delta \tag{0.4}$$

In this case, the coefficients A, B, C, D, E can be calculated by the formulas:

$$A = \sin\varphi\cos\beta \text{ ;(0.5)}$$

$$B = \cos\varphi\sin\beta\cos\gamma \text{ ;} \tag{0.6}$$

$$C = \sin\beta\sin\gamma \text{ ;(0.7)}$$

$$D = \cos\varphi\cos\beta \text{ ;(0.8)}$$

$$E = \sin\varphi\sin\beta\cos\gamma \tag{0.9}$$

where φ – latitude of the terrain at the point of installation of the receiving pad, (deg);

γ – azimuth of the receiving surface, (deg);

δ – the declination angle of the Sun (the angle between the line connecting the centers of the Earth and the Sun and its projection onto the equatorial plane), (rad);

ω – hour angle (the angle measured in the equatorial plane between the projection of the line passing through the center of the Earth and the location of the solar panel, and the projection of the line connecting the centers of the Earth and the Sun), (deg).

The angle of declination is given by the formula:

$$\delta = 0.41 \cdot \sin\left(360 \cdot \frac{N + 284}{365}\right), \tag{0.10}$$

where N – number of the calendar day from the beginning of the year.

Sinus of the angle α is found by the formula

$$\sin\alpha = \sin\varphi \cdot \sin\delta + \cos\varphi \cdot \cos\delta \cdot \cos\omega. \tag{0.11}$$

The scattered solar radiation arriving on the inclined plane is determined by

$$D_{\text{tilt}} = D_{hor}[0.55 + 0.434 \cdot \cos\theta + 0.313(\cos\theta)^2], \tag{0.12}$$

where D_{hor} – is the flux of scattered solar energy (W/ m^2) on the horizontal plane (s = 0), determined by the Berlage formula:

$$D_{hor} = \frac{1}{3}(S_0 - S_{ort})\sin\alpha. \quad (0.13)$$

The scattered solar radiation on the vertical plane is determined from the ratio:

$$D_{ver} = D_{\text{tilt}} + D_{Earth}, \quad (0.14)$$

where $D_{Earth} = 0,47A_{Earth}(S_{gor} + D_{gor})$ - scattered solar radiation reflected from the Earth; D_{ver} - direct solar radiation arriving on the horizontal plane; A_{Earth} - Earth's albedo.

The azimuthal angle of the Sun's position is a solution to the equation [54]:

$$\cos Az = \frac{\sin h\sin\varphi - \sin\delta}{\cos h\cos\varphi}, \quad (0.15)$$

where h – the angle of elevation of the Sun above the horizon, determined by the difference:

$$h = 90^0 - \theta_Z, (\text{град}). \quad (0.16)$$

Zenith angle of the Sun θ_Z is determined by the expression:

$$\theta_Z = \arccos(\sin\varphi\sin\delta + \cos\varphi\cos\delta\cos\omega), \quad (0.17)$$

where ω – hourly angle determining the angular displacement of the Sun during the day. One hour corresponds to π/2 radians or 15 degrees of angular displacement. At noon $\omega = 0$.

Thus, the total solar radiation arriving at an arbitrarily oriented site in clear weather is determined by the ratio:

$$Q_{\text{tilt}}(\varphi,\omega,\gamma,s,N) = S_{\text{tilt}}(\varphi,\omega,\gamma,s,N) + D_{\text{tilt}}(\varphi,\omega,s,N). \quad (0.18)$$

The effect of cloud cover on total radiation flux is expressed by introducing empirical coefficients:

$$Q_{\text{tilt}}(\varphi,\omega,\gamma,s,N) = [S_{\text{tilt}}(\varphi,\omega,\gamma,s,N) + D_{\text{tilt}}(\varphi,\omega,s,N)]\cdot[1-(a+bn)n], \quad (0.19)$$

where n - number of clouds in fractions of one (n = 0 for cloudless sky, n = 1 for solid clouds); b is a conditionally constant coefficient, equal to 0.38; a is a coefficient that depends on the environment and the latitude of the area.

The combination of mathematical formulas and some empirical coefficients describing the geometric position of the sun in the sky allows us to determine the amount of total solar radiation arriving at the surface of the Earth.

2.2 Modeling of the process of solar radiation arrival on the surface of the PV panel

The intensity of solar radiation outside the Earth's atmosphere is almost constant and is equal to 1367 W/m2. However, stochastic factors are influencing the intensity of radiation at the Earth's surface - the state of the atmosphere and the position of the receiving surface. The final task of solar radiation modeling is to determine the value of incoming solar radiation for any day of the year in an arbitrary geographical location of the installation, which causes the modeling of all factors affecting the solar radiation.

The input data are 7 values, which determine the value of the final solar intensity:

1. number of calendar days from the beginning of the year;
2. latitude of the area;
3. tracker availability;
4. Azimuthal angle of installation of the panel;
5. tilt angle of the panel;
6. albedo of the Earth's surface;
7. atmospheric transparency index;

In the Matlab/Simulink software package, the input quantities are set through the Constant parameter block.

One of the objectives of this work is to develop a solar tracker model. If it is part of the installation, the efficiency of the solar panel increases by 40-45%, which allows us to use a smaller number of solar panels to cover the required load. However, the high cost of the solar tracker can be a decisive factor in its installation. In this regard, the model introduces the possibility of having a tracker by azimuth, azimuth, and tilt angle, as well as its absence. In the case of its absence, the known values of the azimuthal angle of installation of the panel and the tilt angle of the panel are used.

The presence of a solar tracker obliges us to know the zenith and azimuth angles of the Sun at each moment (Fig. 2.1). In the developed model, these values are included in the block "Tracker module". This block, using the standard element of the Matlab/Simulink library "Switch", chooses between two options: either from manually entered static terrain parameters, or by equating the azimuthal angle of the panel to the azimuthal angle of the Sun, and the tilt angle of the panel to the ground plane to the angle of elevation of the Sun.

Figure 2.2 shows the block, in which the height of the Sun's elevation above the horizon is determined by formulas (1.10) and (1.11), from Section 2.1.

By formulas (1.10), (1.17) the block "Zenith angle of the Sun" is built in Figure 2.3.

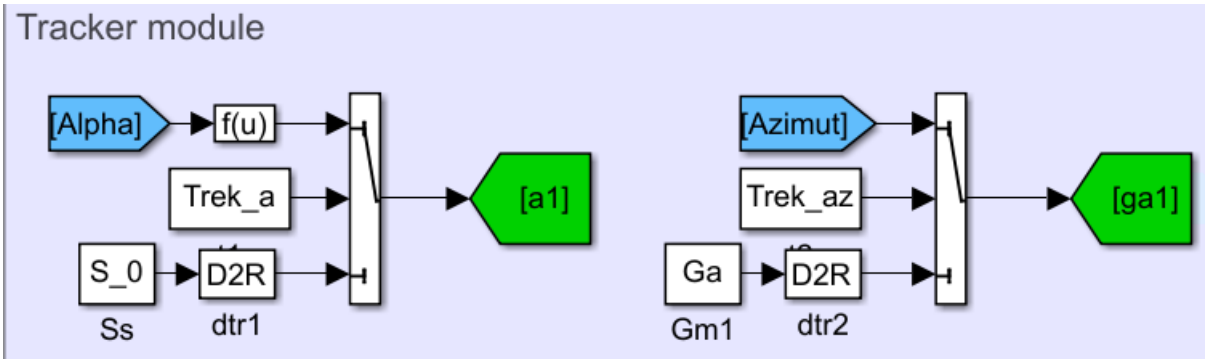

Figure 2.1 - Tracker module

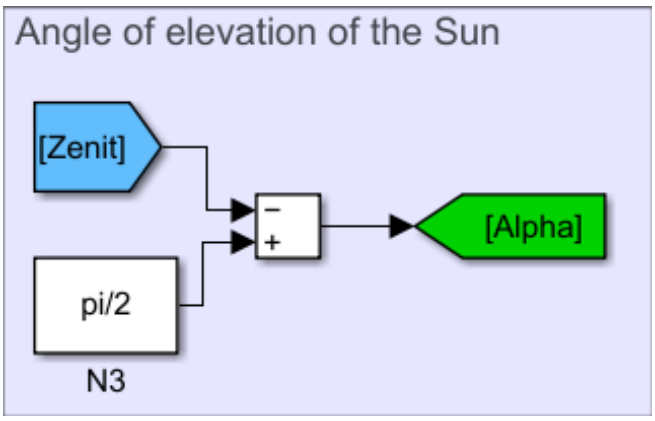

Figure 2.2 - The angle of elevation of the Sun, according to formulas 1.16, 1.17

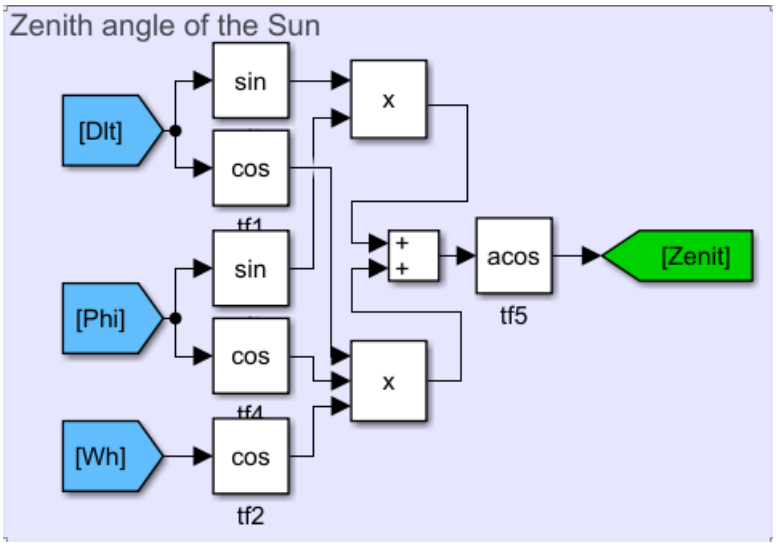

Figure 2.3 - The zenith angle of the Sun, according to formula 1.17

Figure 2.4 shows the block "Azimuthal angle of the Sun". It was built on the basis of calculations from the block "Angle of Ascent of the Sun" and formulas (1.15).

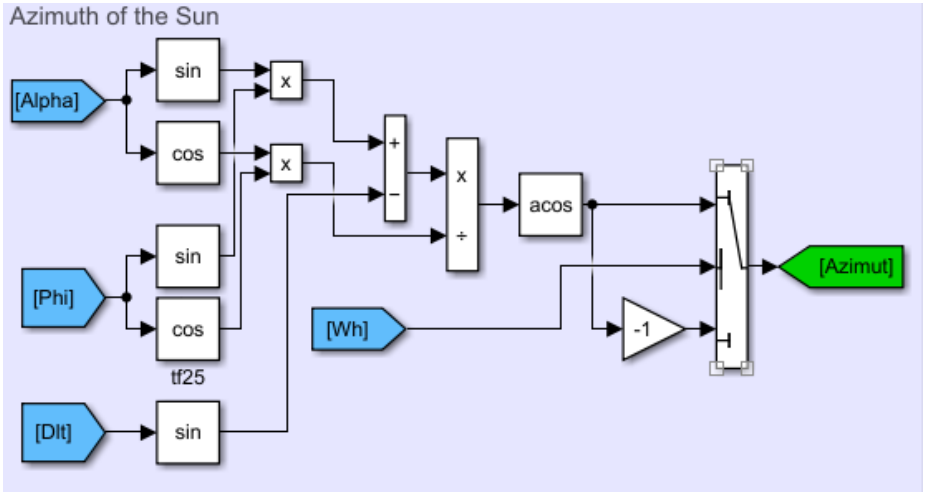

Figure 2.4 - Azimuth of the Sun, according to formula 1.15

The last block "Radiation" was made based on calculations of all previous blocks, as well as formulas (1.1) - (1.19), and is shown in Figure 2.5.

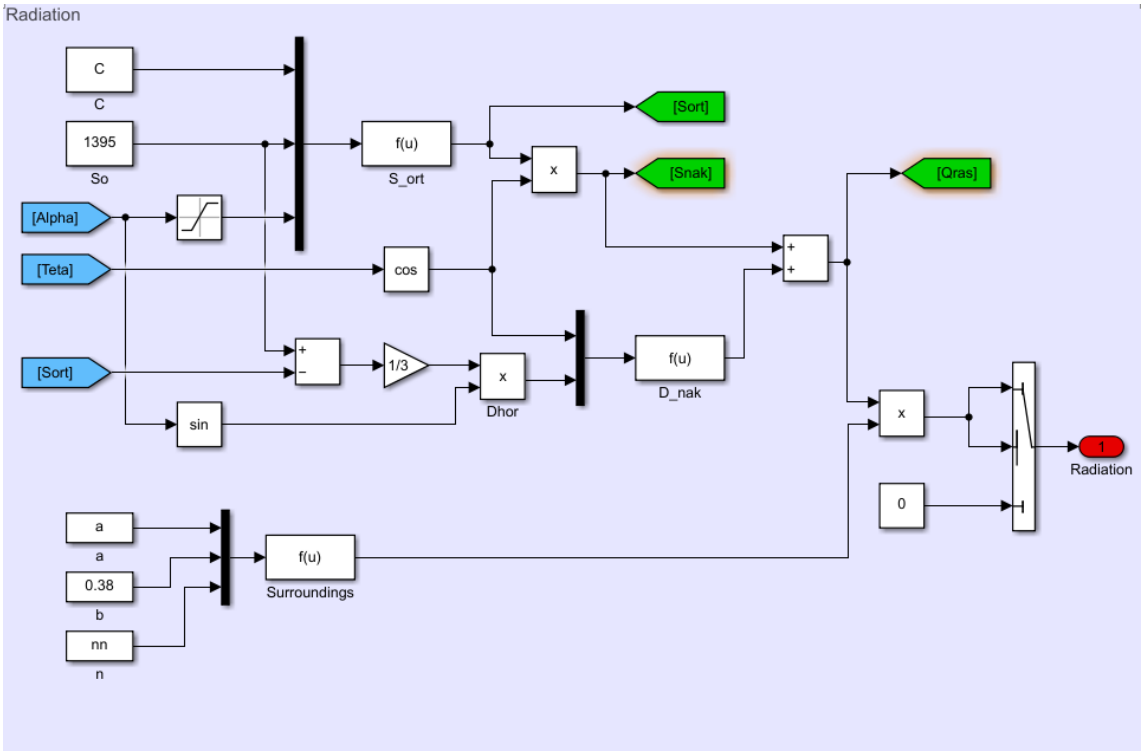

Figure 2.5 - The output value of solar radiation, according to formulas (1.1) - (1.19)

The possibility to study theϕ fast processes of solar radiation changes is provided by the empirical coefficients integrated into the "Radiation" block (Figure 2.5), which simulate cloudiness.

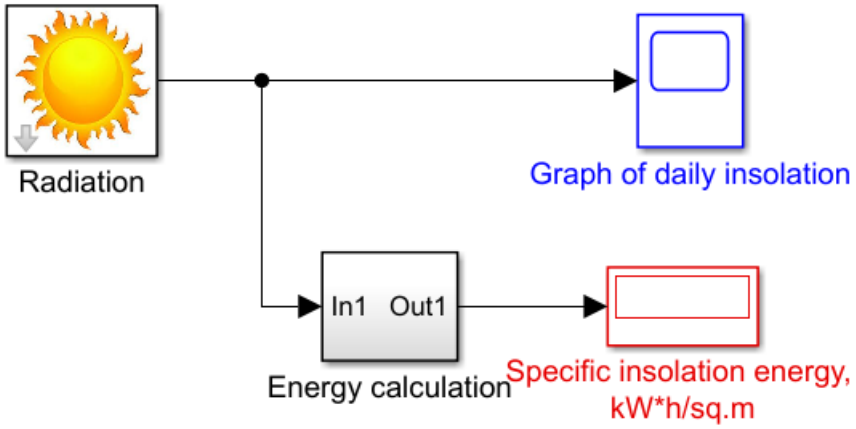

Figure 2.6 - General view of the program subsystem

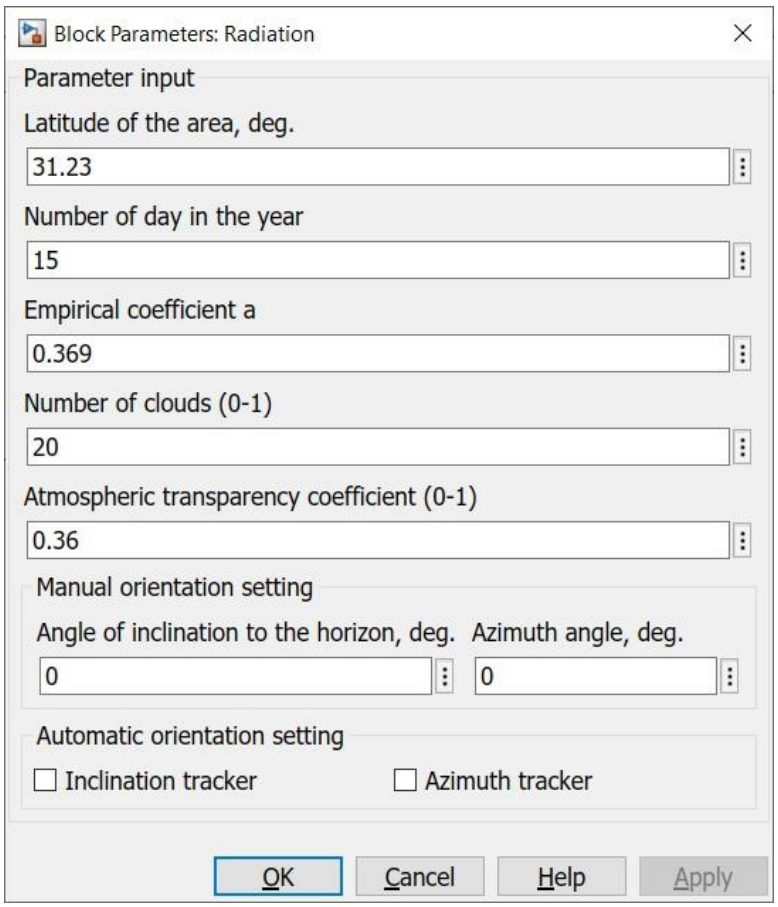

Figure 2.7 - Input window for initial parameters

The model was formed into a subsystem (Figure 2.6) with the possibility of changing the input parameters to calculate the value of radiation arrival on any terrain (Figure 2.7), as well as for any day of the year. The possibility to set the operation mode of the solar tracker allows us to estimate its efficiency in the given climatic conditions.

2.3 Verification of the model

The performance of the model was tested for a characteristic day at each time of the year. The characteristic day was the 15th day of January, April, July, and November, respectively. Thus, by determining the area under the curve of insolation, we obtained the average value of the specific energy of insolation for each time of the year in Shanghai, Brno, and the Alexandrovskoe village.

To compare the obtained values, the NASA database was taken and the average value of specific energy of insolation by seasons was determined.

The data obtained for the selected points are summarized in Tables 2.1-2.3.

The error of calculation by the model was also determined by the following formula:

$$\Delta = 100\% - \frac{Q_{Sim} \cdot 100\%}{Q_{NASA}},$$

where Q_{Sim} - data obtained by simulation, kW/ m^2;

Q_{NASA} - data obtained from NASA database, kW/ m^2.

Thus, the calculation error using the model for Shanghai in winter of 2020 will be as follows:

$$\Delta = 100\% - \frac{Q_{Sim} \cdot 100\%}{Q_{NASA}} = 100\% - \frac{1,517 \cdot 100}{1,506} = 0,73\%.$$

Table 2.1 - Summary data of insolation indicators in Shanghai for 2020

Time of the year	Winter	Spring	Summer	Autumn
NASA data, kW*h/ m^2	1.506	3.902	4.864	4.000
Simulation values, kW*h/ m^2	1.517	4.216	4.812	4.062
Error rate, %	0.760	8.042	1.072	1.550

Table 2.2 - Summary data of insolation indicators in Brno for 2020

Time of the year	Winter	Spring	Summer	Autumn
NASA data, kW*h/ m^2	1.045	4.239	4.609	2.019
Simulation values, kW*h/ m^2	1.01	4.324	4.673	1.991
Error rate, %	3.354	2.002	1.395	1.398

Table 2.3 - Summary data of insolation indicators in Alexandrovskoye village for 2020

Time of the year	Winter	Spring	Summer	Autumn
NASA data, kW*h/ m^2	1.817	6.186	5,413	2.854
Simulation values, kW*h/ m^2	1.657	5.763	5.13	2.603
Error rate, %	8.806	6.839	5.229	8.795

2.4 The final result of chapter 2

Thus, we can conclude that the accuracy of the developed model is acceptable. The analysis of obtained results showed that for the majority of considered parameter changes the model adequately shows the diurnal variations of solar radiation intensity. The discrepancy of readings as compared with the NASA reference database for Shanghai is on average 3%, for Brno - about 2%, for Alexandrovskoe village - 8%.

3. Simulation of the modes of operation of the tracking installation

3.1 Mode of operation without a tracker

The primary task in the application of solar panels for power generation is the optimal position of the receiving pad. By the position of the receiving pad is meant its inclination in the vertical plane - relative to the Earth's surface - as well as its orientation in the horizontal plane (azimuthal angle).

As a rule, in stationary solar installations, the receiving pad in the horizontal plane is oriented to the South. But the angle of inclination relative to the Earth's surface is chosen experimentally.

To determine the optimal angle of inclination, the following study was conducted. For three geographical points Shanghai (φ = 31,23°), Brno (φ = 49,18°) and Alexandrovskoe (φ = 58,31°), chosen according to their location in low, middle and high latitudes, the power of solar radiation arriving at the receiving surface was determined for each month of the year using the developed model of solar radiation arrival. The limits of variation of the tilt angle are from 0 to 90 degrees, with a step of 10 degrees.

Below is a table with data on geographical points, for which the simulation was performed.

Table 3.1 - Data on geographical points

City	Shanghai				Brno				Alexandrovskoye			
Coordinates	31.23				49.18				58.31			
Time of year	W	S	S	A	W	S	S	A	W	S	S	A
a	0.369				0.398				0.367			
n	20	30	35	30	50	25	40	50	50	50	50	60
C	0.36	0.37	0.39	0.37	0.34	0.49	0.43	0.34	0.38	0.5	0.44	0.28

The empirical coefficient a was taken from [55]. It differs on land and sea and depends on the latitude of the area. The coefficient n shows the percentage of cloudiness in the area in question. The value of this parameter was averaged over 15 years of observations for each time of year. The observation data were taken from [56]. C is the atmospheric transparency coefficient, the values of which were also averaged for each time of year, based on NASA observations for 15 years [57].

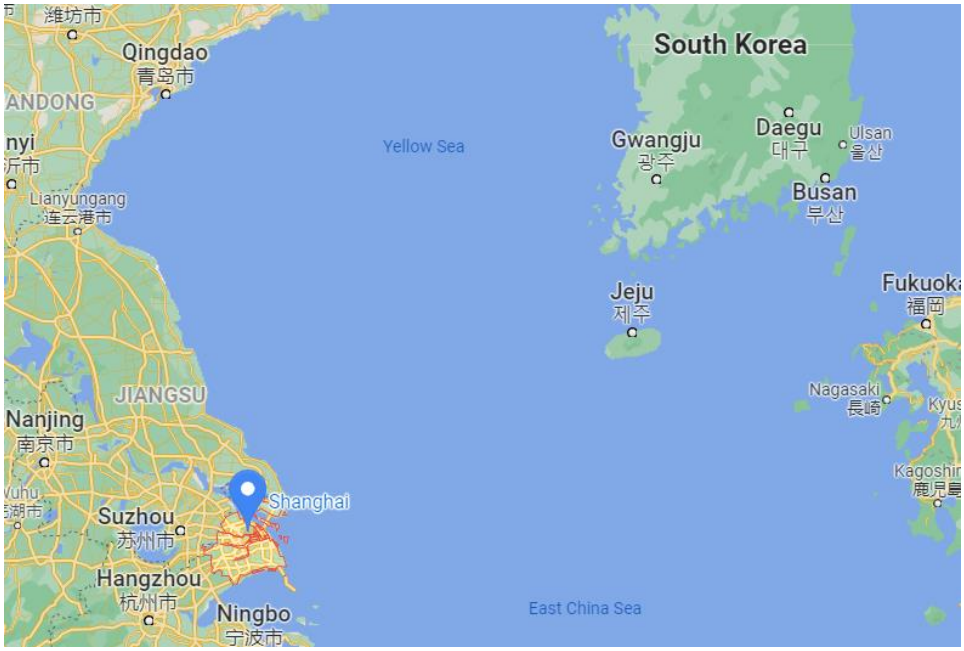

Figure 3.1 - Geographical location of Shanghai

To determine the energy of solar radiation, we chose a characteristic day in each month of the year (the 15th day). Thus, simulated days for winter: 349, 15, 46; for spring: 75, 105, 136; for summer: 166, 196, 227 and for autumn: 258, 288, 320.

The results of the study for Shanghai are presented in the table below. From the data we can conclude that the average value of the slope angle for the winter period is 57 degrees, for the spring period - 20 degrees, for the summer period - 3 degrees, and autumn period - 40 degrees. The average value of the slope angle for the year is 30 degrees, which is approximately equal to the latitude of the area

Table 3.2 - Optimal panel angle for Shanghai

Angle of inclination	Radiation energy, kWh/m^2											
	January	February	March	April	May	June	July	August	September	October	November	December
0	3.432	4.503	5.476	6.81	7.659	7.644	7.517	6.899	6.051	4.658	3.465	3.686
10	4.212	5.241	6.018	7.072	7.641	7.484	7.416	7.031	6.491	5.305	4.186	4.462
20	4.879	5.834	6.391	7.132	7.405	7.114	7.105	6.962	6.747	5.805	4.794	5.118
30	5.41	6.262	6.581	6.987	6.963	6.553	6.6	6.696	6.81	6.14	5.269	5.631
40	5.788	6.511	6.582	6.643	6.332	5.822	5.921	6.242	6.676	6.298	5.593	5.983
50	5.998	6.571	6.393	6.112	5.536	4.95	5.093	5.617	6.351	6.274	5.756	6.136
60	6.034	6.44	6.021	5.413	4.603	3.971	4.148	4.844	5.847	6.069	5.752	6.163
70	5.895	6.124	5.479	4.57	3.569	2.923	3.124	3.95	5.18	5.691	5.581	5.984
80	5.584	5.633	4.787	3.612	2.477	1.856	2.064	2.968	4.374	5.151	5.248	5.632
90	5.114	4.984	3.967	2.573	1.383	0.843	1.033	1.936	3.457	4.471	4.767	5.12

A similar study was carried out for points in Brno and the village Alexandrovskoe. The results of the simulation are presented below.

Figure 3.2 - Geographical location of the city of Brno

Table 3.3 - Optimal panel angle for the city of Brno

Angle of inclination	Radiation energy, kWh/ m^2											
	January	January	January	January	January	January	January	January	January	January	January	January
0	1.005	1.818	3.531	5.365	6.909	6.95	6.688	5.511	3.731	2.198	1.183	0.821
10	1.473	2.391	4.179	5.895	7.217	7.104	6.897	5.924	4.295	2.792	1.682	1.249
20	1.906	2.902	4.719	6.264	7.327	7.065	6.918	6.174	4.742	3.313	2.141	1.647
30	2.288	3.334	5.13	6.458	7.239	6.843	6.755	6.251	5.054	3.743	2.542	2.004
40	2.608	3.673	5.399	6.472	6.957	6.445	6.415	6.154	5.222	4.068	2.874	2.305
50	2.854	3.907	5.514	6.304	6.491	5.884	5.909	5.886	5.239	4.275	3.124	2.542
60	3.018	4.028	5.472	5.96	5.856	5.18	5.254	5.456	5.105	4.359	3.284	2.705
70	3.094	4.031	5.275	5.453	5.077	4.357	4.474	4.88	4.824	4.316	3.348	2.789
80	3.079	3.917	4.93	4.8	4.181	3.447	3.597	4.178	4.407	4.147	3.313	2.792
90	2.973	3.689	4.449	4.026	3.203	2.486	2.659	3.376	3.867	3.859	3.182	2.712

From the data, you can conclude that for winter the average value of the angle of inclination - 73 degrees, for spring - 37 degrees, for summer - 20 degrees, and for autumn - 60 degrees. The average value of the slope angle for the year is 48 degrees, which is approximately equal to the latitude of the area.

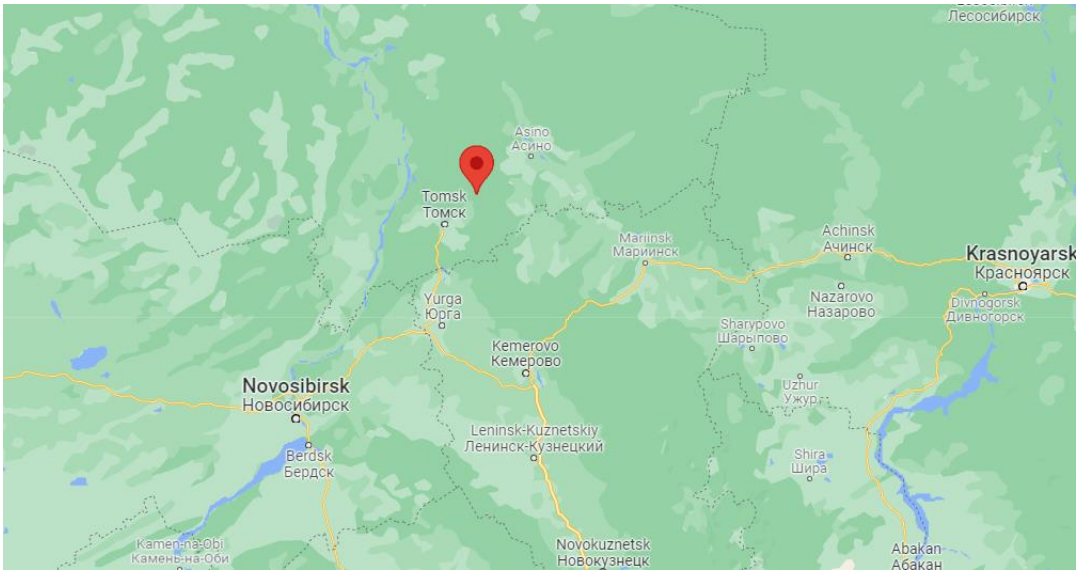

Figure 3.3 - Geographical location of Alexandrovskoye village

Table 3.4 - Optimal panel angle for Alexandrovskoe village

Angle of inclination	Radiation energy, kWh/ m^2											
	January	January	January	January	January	January	January	January	January	January	January	January
0	0.338	0.973	2.051	3.683	5.208	5.945	5.6	4.446	2.763	1.289	0.46	0.222
10	0.6	1.425	2.572	4.185	5.559	6.182	5.894	4.918	3.352	1.813	0.795	0.424
20	0.849	1.843	3.029	4.577	5.763	6.265	6.036	5.257	3.85	2.29	1.112	0.618
30	1.078	2.215	3.407	4.845	5.821	6.197	6.028	5.454	4.239	2.706	1.4	0.798
40	1.279	2.526	3.693	4.979	5.727	5.978	5.869	5.503	4.508	3.045	1.649	0.957
50	1.445	2.767	3.875	4.975	5.484	5.611	5.56	5.4	4.646	3.298	1.852	1.09
60	1.57	2.929	3.947	4.832	5.098	5.107	5.111	5.149	4.649	3.454	2.002	1.192
70	1.649	3.006	3.907	4.555	4.582	4.482	5.536	4.758	4.517	3.51	2.093	1.26
80	1.68	2.995	3.756	4.154	3.955	3.758	3.856	4.24	4.254	3.462	2.123	1.291
90	1.662	2.897	3.499	3.643	3.239	2.962	3.096	3.614	3.869	3.313	2.089	1.284

From the data, you can conclude that the average value of the angle of inclination for the winter period - 77 degrees, for spring - 57 degrees, for summer - 27 degrees, and for autumn - 70 degrees. The average value of the slope angle for the year is 55 degrees, which is approximately equal to the latitude of the area.

Thus, when determining the optimum angle of inclination of the reception site, it turned out that the average value of this angle in all cases is approximately equal to the latitude of the terrain in which the system is supposed to be installed. Besides, according to the obtained data, it is clear that as the latitude of the terrain increases, the angle of slope of the receiving pad in each season also increases.

The revealed regularities allow us to conclude that when using a stationary solar installation, as well as when there is no possibility of monthly or seasonal adjustment of the angle of inclination of the receiving pad, it can be set equal to the latitude of the terrain.

3.2 Mode of operation with a single-axis tracker by the azimuth angle

In this mode, the azimuth angle is automatically corrected by the tracking system. The azimuthal angle of the panel is equal to the azimuthal angle of the Sun. The tilt angle is corrected manually according to the previously selected optimum angle.

Figure 3.4 shows graphs of solar radiation for Shanghai by the characteristic day of each month.

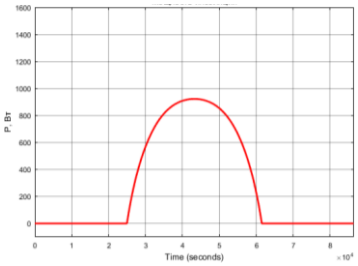

January

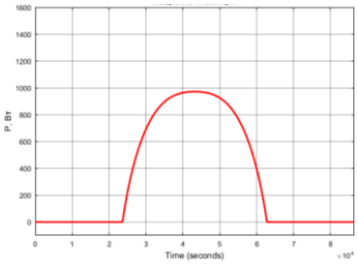

February

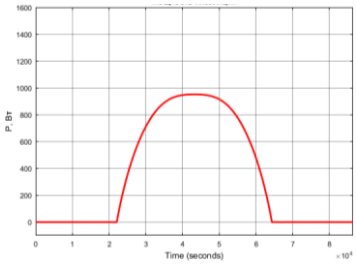

March

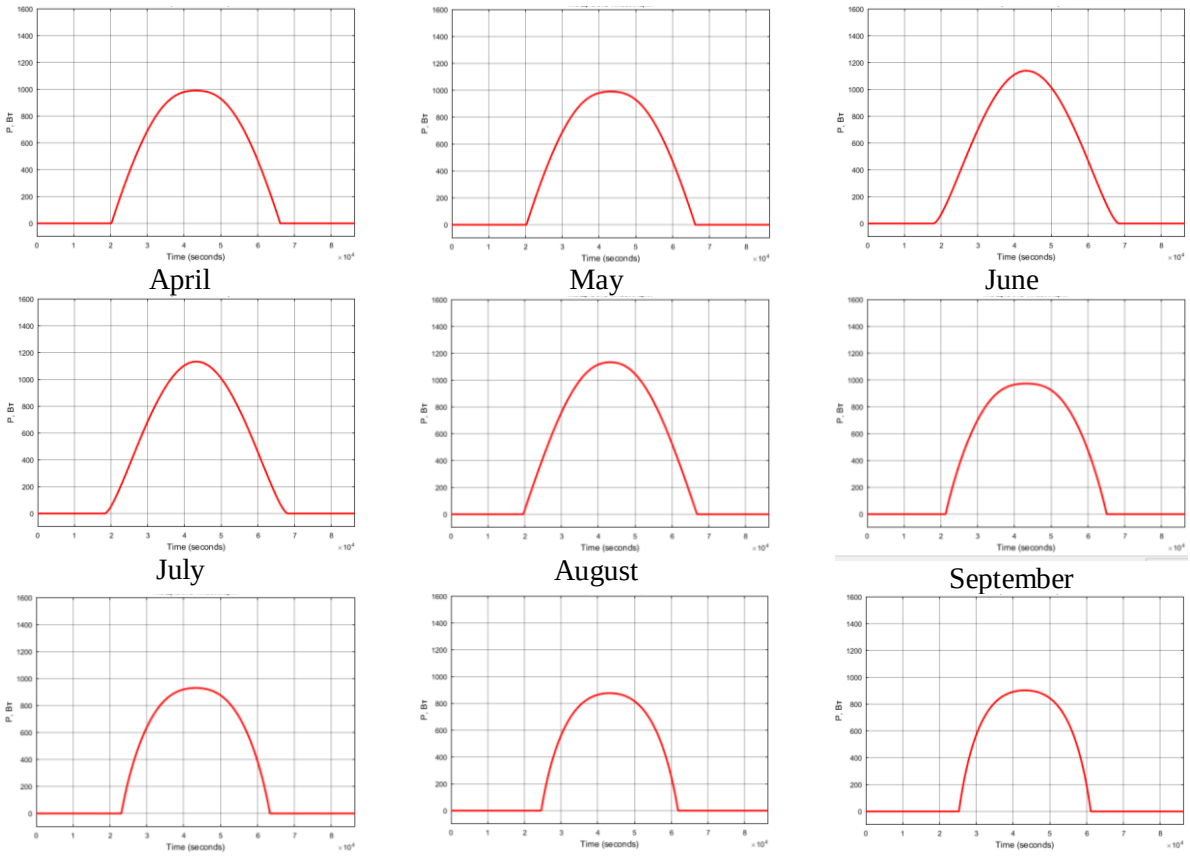

Figure 3.4 - Arrival of insolation with the azimuthal tracker of Shanghai by months of the year

Table 3.1 shows the results of calculating the radiation energy for Shanghai.

Table 3.1 - Radiation energy with azimuth tracker Shanghai

Month	January	February	March	April	May	June
Angle of inclination	60	50	40	20	0	0
Energy, kWh/m2	6.942	8.018	8.358	8.591	8.659	8.824
Month	July	August	September	October	November	December
Angle of inclination	0	10	30	40	50	60
Energy, kWh/m2	9.214	9.738	8.478	7.634	6.745	6.812

The total power of solar radiation for the year will be 2973.7 kW/m2, which is 21.2% more than for the stationary installation with optimally chosen angles of inclination and azimuth angle = 0 degrees, and 17.011% more than for the installation with a tracker by inclination and azimuth angle = 0 degrees.

Figure 3.5 shows graphs of solar radiation for Brno by characteristic day of each month.

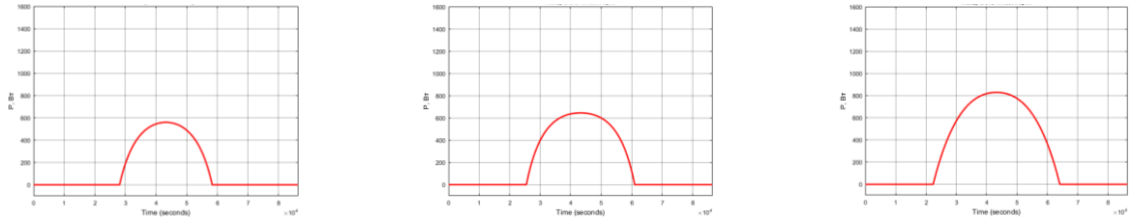

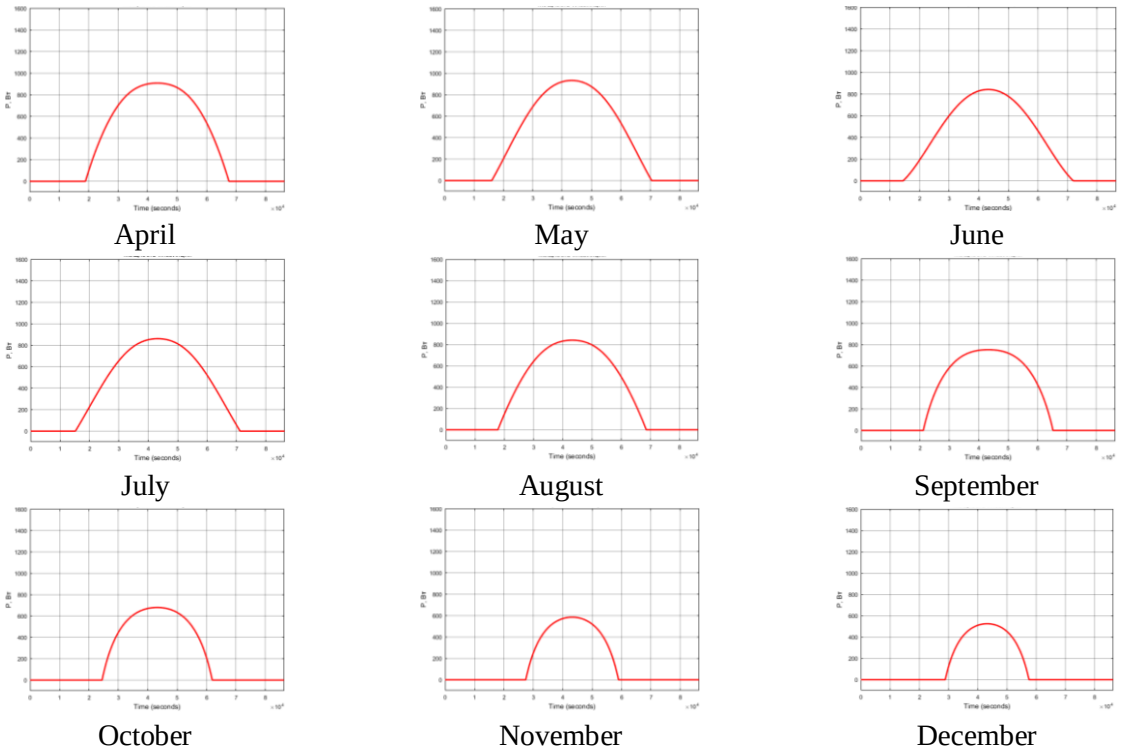

Figure 3.5 - Arrival of insolation with azimuth tracker G.Brno by month of the year

Table 3.2 - Radiation energy with azimuth tracker of Brno

Month	January	February	March	April	May	June
Angle of inclination	70	70	50	40	20	10
Energy, kWh/m2	3.453	4.81	6.9	8.672	9.029	8.068
Month	July	August	September	October	November	December
Angle of inclination	20	30	50	60	70	80
Energy, kWh/m2	8.656	8.118	6.89	5.283	3.791	3.082

The total power of solar radiation for the year will be 2352.2 kW/m2, which is 23.95% more than for stationary installation with optimally chosen angles of inclination and azimuthal angle = 0 degrees. Figure 3.6 shows graphs of solar radiation arrival for Alexandrovskoye village by characteristic day of each month.

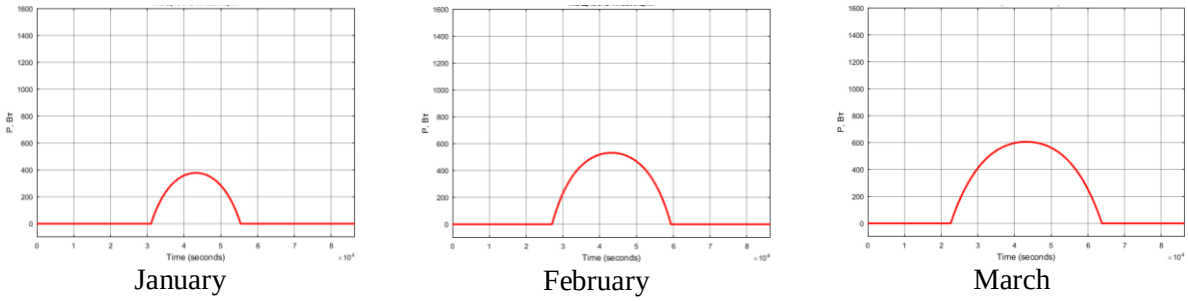

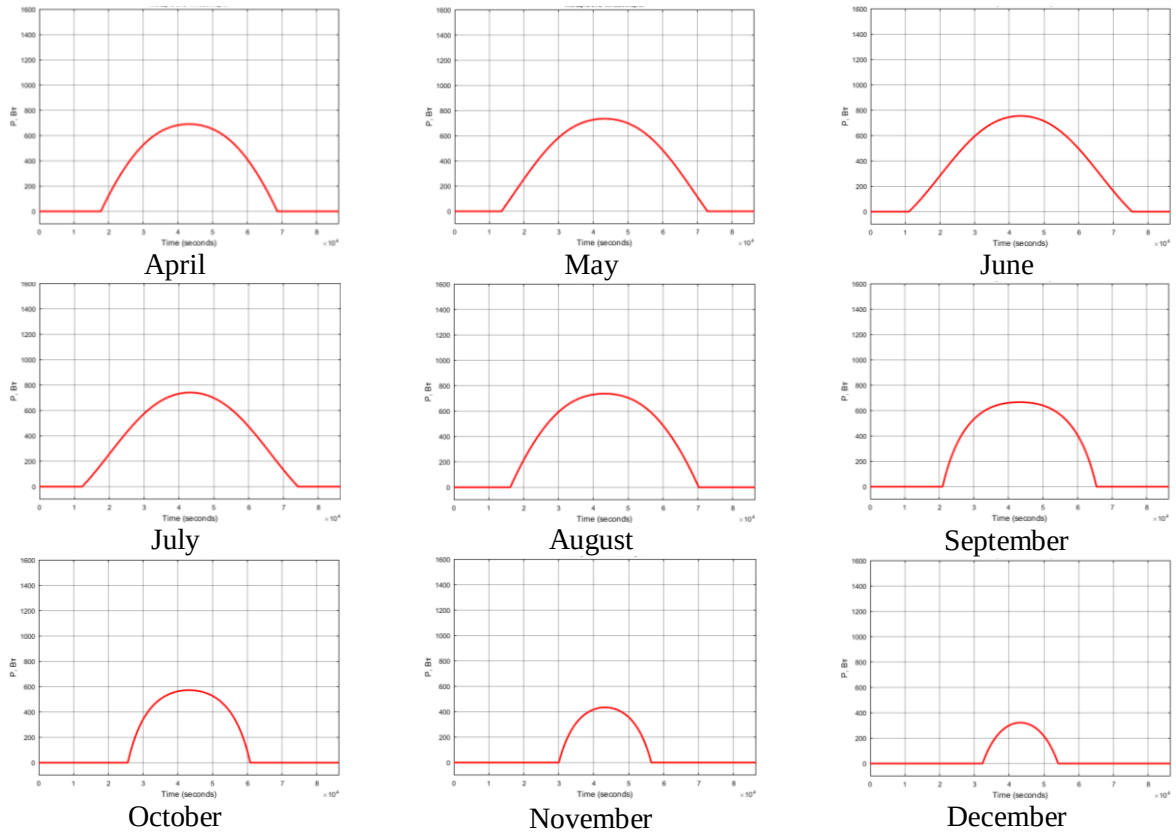

Figure 3.6 - Insolation arrival with the azimuthal tracker in Alexandrovskoye by months of the year

Table 3.3 shows the results of the calculation of the radiation energy for Alexandrovskoye village.

Table 3.3 - Radiation energy with the azimuthal tracker in Alexandrovsky village Alexandrovskoye

Month	January	February	March	April	May	June
Angle of inclination	80	70	60	40	30	20
Energy, kWh/m2	1.802	3.444	4.954	6.683	7.909	8.308
Month	July	August	September	October	November	December
Angle of inclination	20	40	60	70	80	80
Energy, kWh/m2	7.911	7.664	6.256	4.186	2.318	1.362

The total power of solar radiation for the year will be 1909.4 kW/m2, which is 28.7% more than the stationary installation with optimally chosen angles of inclination and azimuthal angle = 0 degrees.

3.3 Mode of operation with a single-axis tracker by a tilt angle

In this mode, the tilt angle is automatically corrected by the tracking system, it is equal to the angle of elevation of the Sun. The azimuth angle is equal to zero.

Table 3.4 - Energy of radiation with tracker by tilt angle Shanghai, kWh/m2

January	February	March	April	May	June
6.054	6.605	6.387	7.254	7.861	7.905
July	August	September	October	November	December
8.172	7.748	7.259	6.831	5.778	5.888

The total power of solar radiation for the year will be 2541.4 kW/m2, which is 3.5% more than for stationary installation with optimally chosen angles of inclination and azimuthal angle = 0 degrees.

Figure 3.7 shows graphs of solar radiation arrival for Shankha y by characteristic day of each month.

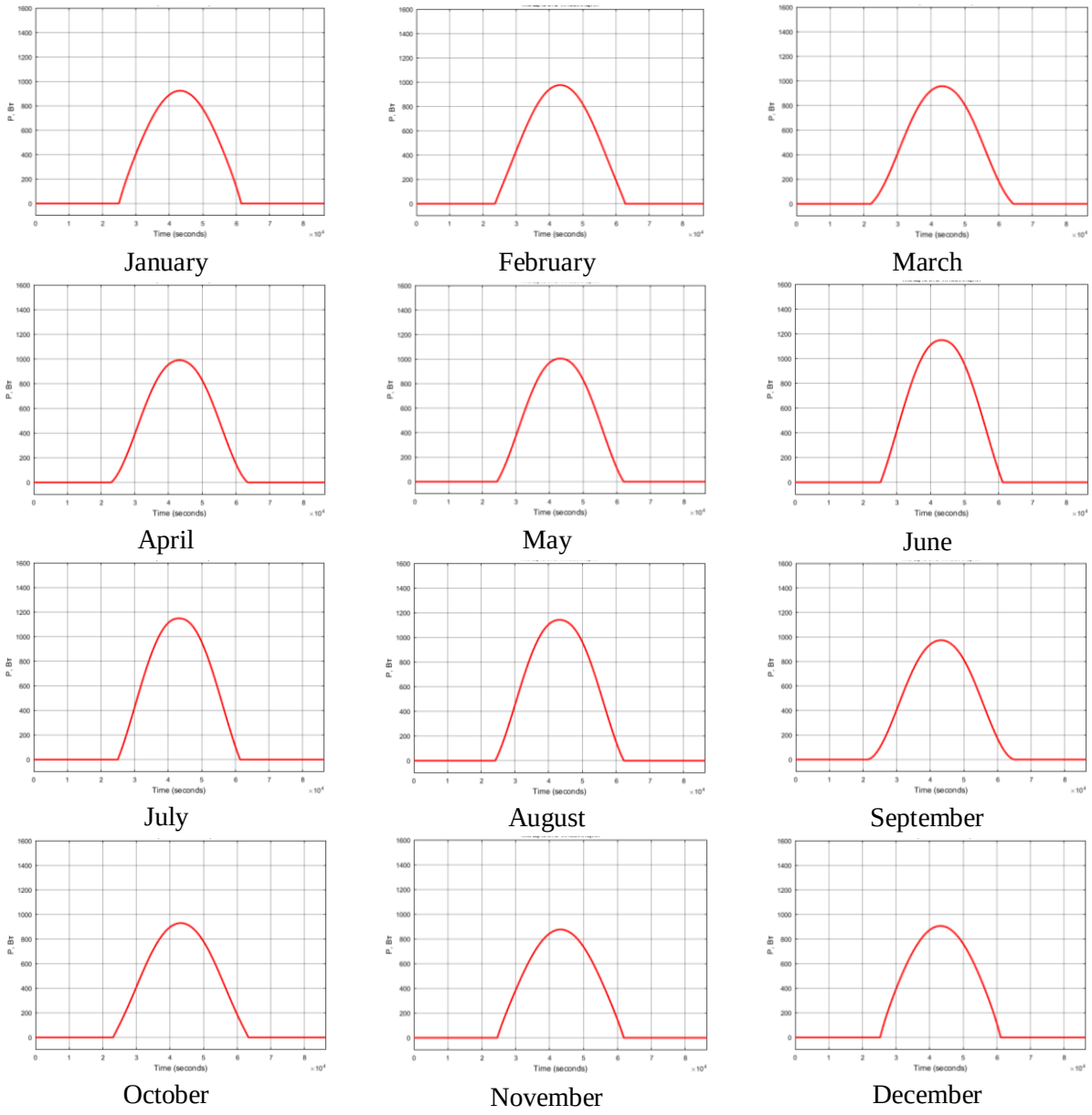

Figure 3.7 - Arrival of insolation with the tracker by the tilt angle of Shanghai by months of the year

Table 3.5 - Energy of insolation with tracker by tilt angle Brno, kWh/m2

January	February	March	April	May	June
3.103	4.044	5.453	6.161	6.702	6.509
July	August	September	October	November	December
6.346	5.683	4.699	4.352	3.353	2.805

The total power of solar radiation for the year will be 1799.6 kW/m2, which is 5.2% more than for stationary installation with optimally chosen angles of inclination and azimuthal angle = 0 degrees.

Figure 3.8 shows graphs of solar radiation arrival for Brno by characteristic day of each month.

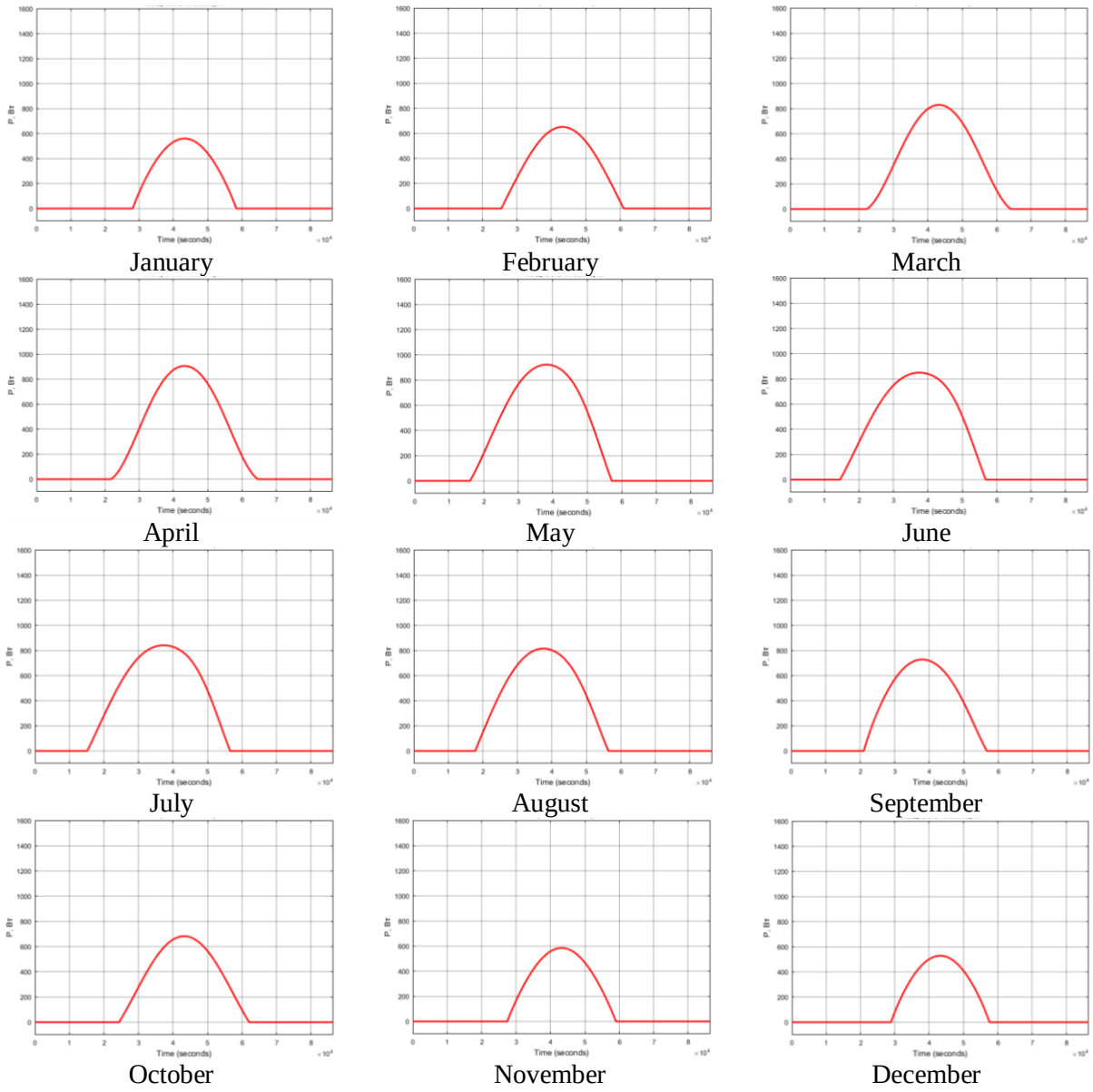

Figure 3.8 - Insolation with a tracker by the tilt angle of Brno by months of the year

Table 3.6 - Energy of insolation with tracker by tilt angle Brno, kWh/m2

January	February	March	April	May	June
1.682	3.014	3.925	4.828	5.358	5.869
July	August	September	October	November	December
5.697	5.195	4.589	3.509	2.124	1.294

The total power of solar radiation for the year will be 1430.1 kW/m2, which is 3.6% more than for stationary installation with optimally chosen angles of inclination and azimuthal angle = 0 degrees.

Figure 3.9 shows graphs of solar radiation arrival for Alexandrovskoye village by characteristic day of each month.

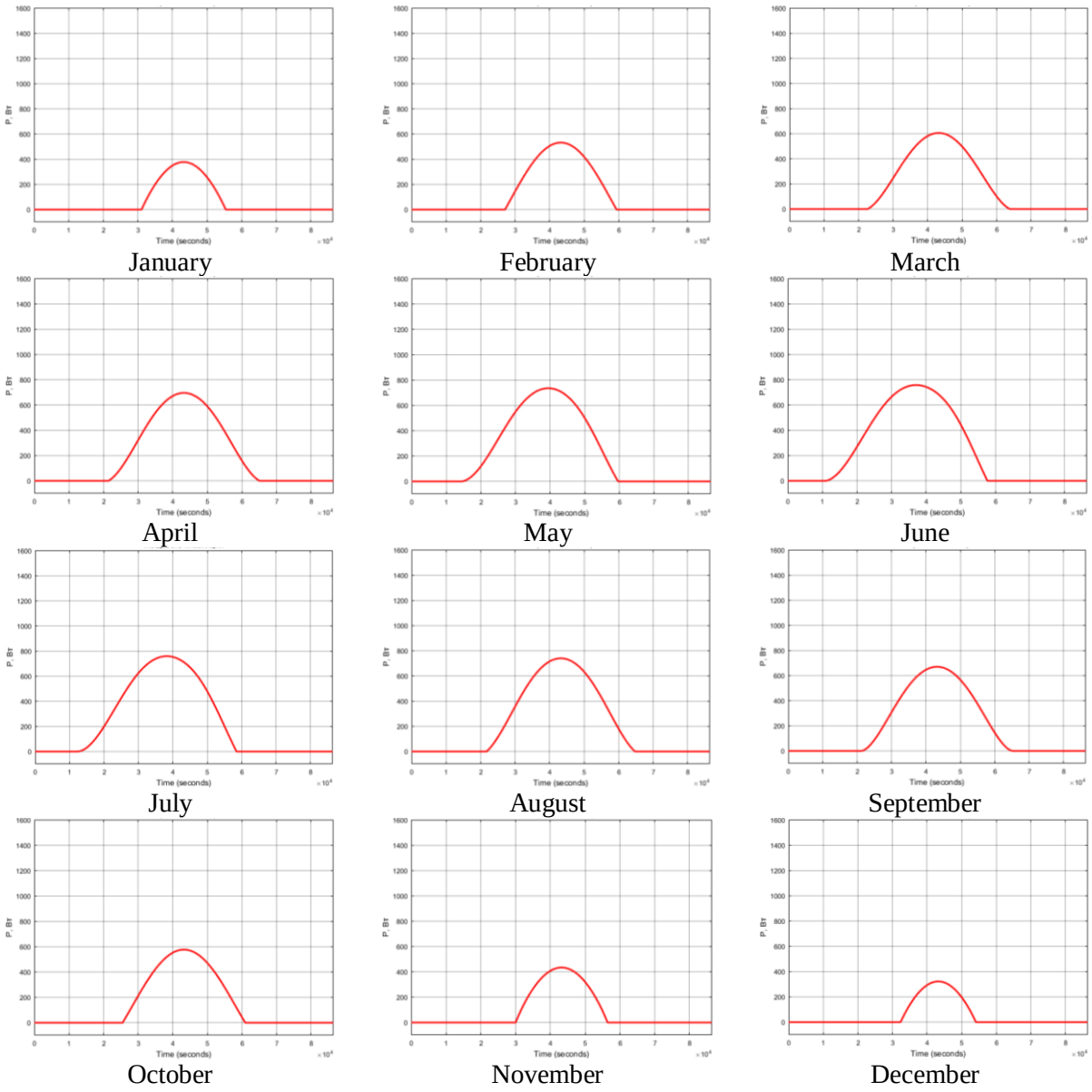

Figure 3.9 - The arrival of insolation with the tracker on the angle of inclination of Alexandrovskoye village by months of the year

3.4 Mode of operation with a two-axis tracker

In the mode under consideration, the azimuthal and tilt angles are corrected automatically by the tracking system, equating them to the azimuthal angle and the angle of elevation of the Sun, respectively.

Table 3.7 - Energy of radiation with tracker by tilt angle Shanghai, kWh/m2

January	February	March	April	May	June
7.206	8.253	8.797	9.92	10.7	10.81
July	August	September	October	November	December
10.81	13.21	12.48	10.278	8.596	7.877

Figure 3.10 shows graphs of solar radiation for Shanghai y by characteristic day of each month.

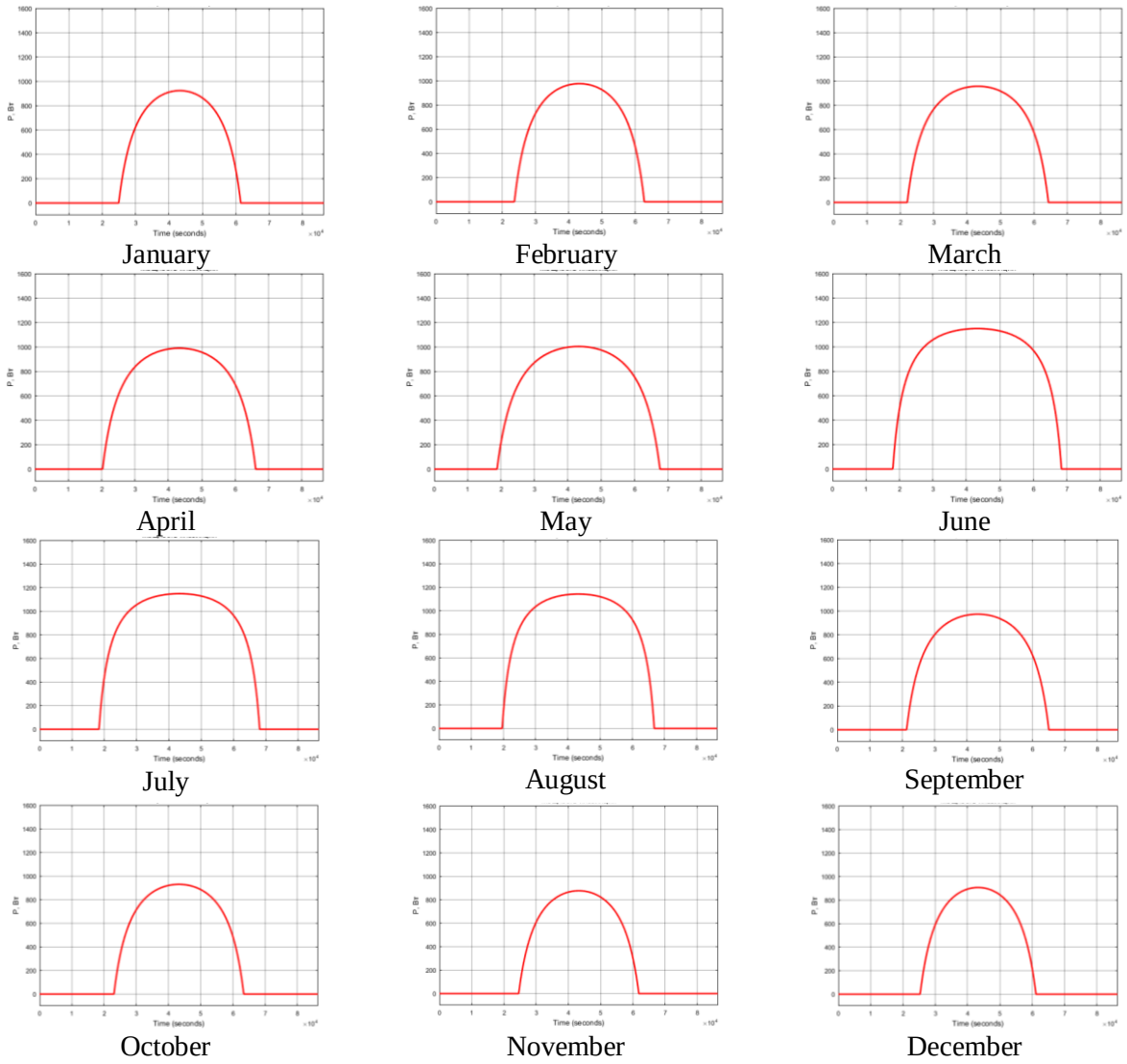

Figure 3.10 - Arrival of insolation with a two-axis tracker Shanghai by months of the year

The total power of solar radiation for the year will be 3494,219 kW/m2, which is 42,364% more than for the stationary installation with optimally selected tilt angles and azimuth angle = 0 deg, 37,493% more than for the automatic selection of the tilt angle, and 17,504% more than for the automatic selection of the azimuth angle.

Table 3.8 - Energy of radiation with tracker by tilt angle Brno, kWh/m2

January	February	March	April	May	June
3.478	4.843	7.143	9.17	10.67	10.5
July	August	September	October	November	December
10.22	9.026	6.424	5.372	3.814	3.095

Figure 3.11 shows graphs of solar radiation for Brno by characteristic day of each month.

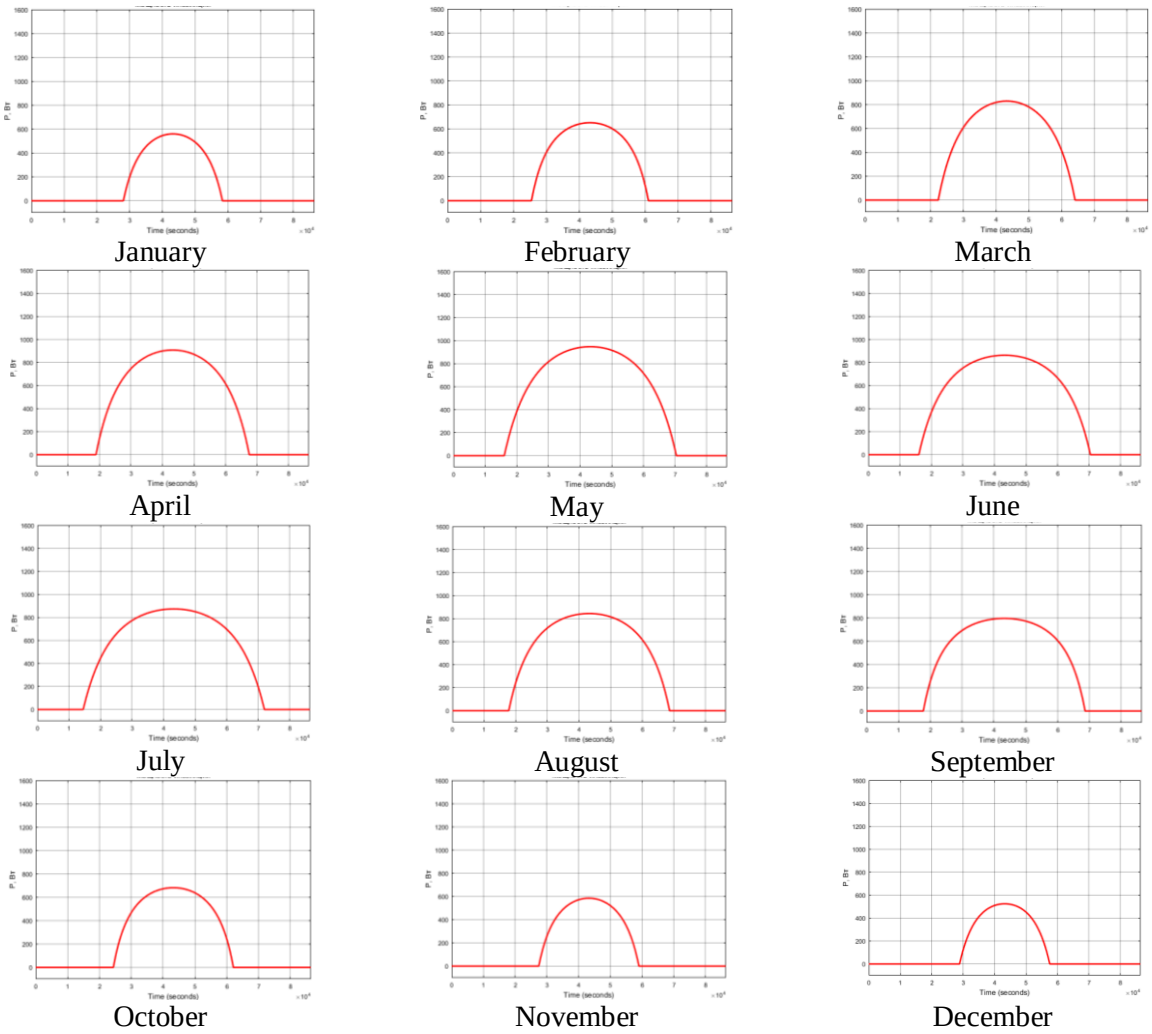

Figure 3.11 - Arrival of insolation with a two-axis tracker Brno by months of the year

The total power of solar radiation for the year will be 2547.1 kW/m2, which is 34.2% more than for the stationary installation with optimally selected tilt angles and azimuth angle = 0 deg, 41.5% more than for the automatic selection of the tilt angle, and 8.3% more than for automatic selection of the azimuth angle.

Table 3.9 - Energy of radiation with the tracker by tilt angle in Alexandrovskoye village, kWh/m2

January	February	March	April	May	June
1.804	3.472	5.042	7.221	8.912	10.14
July	August	September	October	November	December
9.733	8.217	6.358	4.213	2.321	1.365

Figure 3.12 shows graphs of solar radiation for Brno by characteristic day of each month.

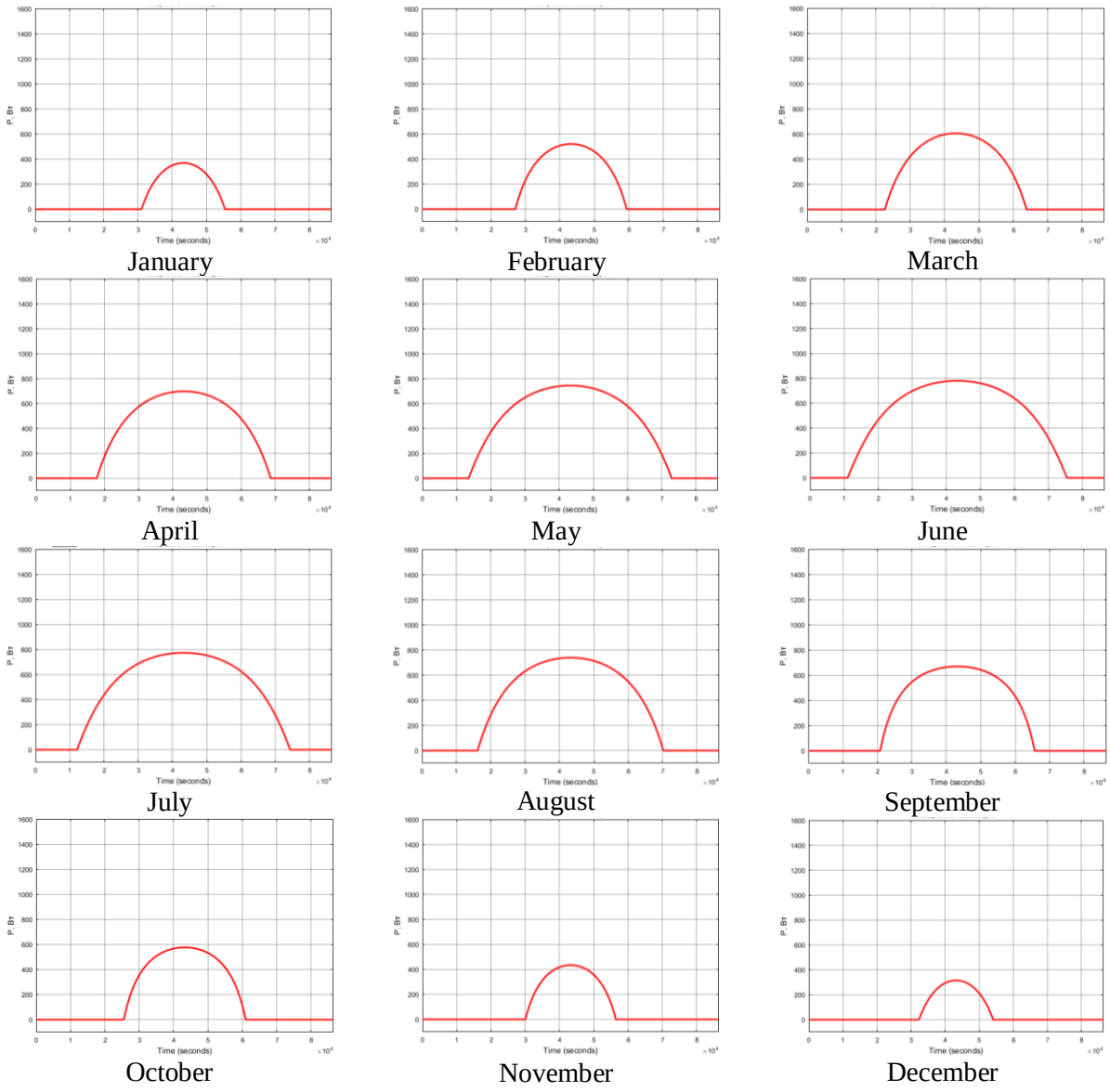

Figure 3.12 - Income of insolation with a two-axis tracker of Alexandrovskoye village by months of the year

The total power of solar radiation for the year will be 2092,8 kW/m2, which is 41,1% more than for stationary installation with optimally selected tilt angles and azimuth angle = 0 degrees, 46,3% more than for automatic selection of the tilt angle, and 9,6% more than for automatic selection of the azimuth angle.

3.5 The final result of chapter 3

To compare the different modes of operation, the modes of a single-axis tracker by azimuthal angle and by surface tilt angle, as well as a two-axis tracker that combines positioning by both of the above angles were chosen.

Thus, the use of a two-axis positioning system is most appropriate in equatorial latitudes, azimuthal tracker - in latitudes close to northern latitudes. The tilt-tracker application does not give a significant increase in production, which indicates that its application is unprofitable.

The following conclusions can be drawn from the results of the simulation:

Table 3.10 - Energy production growth rates in percentage ratio

	Shanghai	Brno	Alexandrovskoe
Two-axis tracker	17,5%	8,3%	9,6%
Azimuth tracker	17%	19,5%	20%
Angle Tracker	3,5%	3,6%	7,3%

4. Building a power supply system using solar trackers

4.1 Equipment overview

For further consideration of the application of the developed model, it is necessary to select the equipment needed to generate electricity from solar radiation.

The choice of equipment is made based on the operating mode of PVS: stand-alone or grid mode. Stand-alone mode of operation implies complete coverage of the consumed energy at the expense of PVS generation. Network mode is based on the joint parallel operation of the PVS and the power grid of the city. (Figure 4.1)

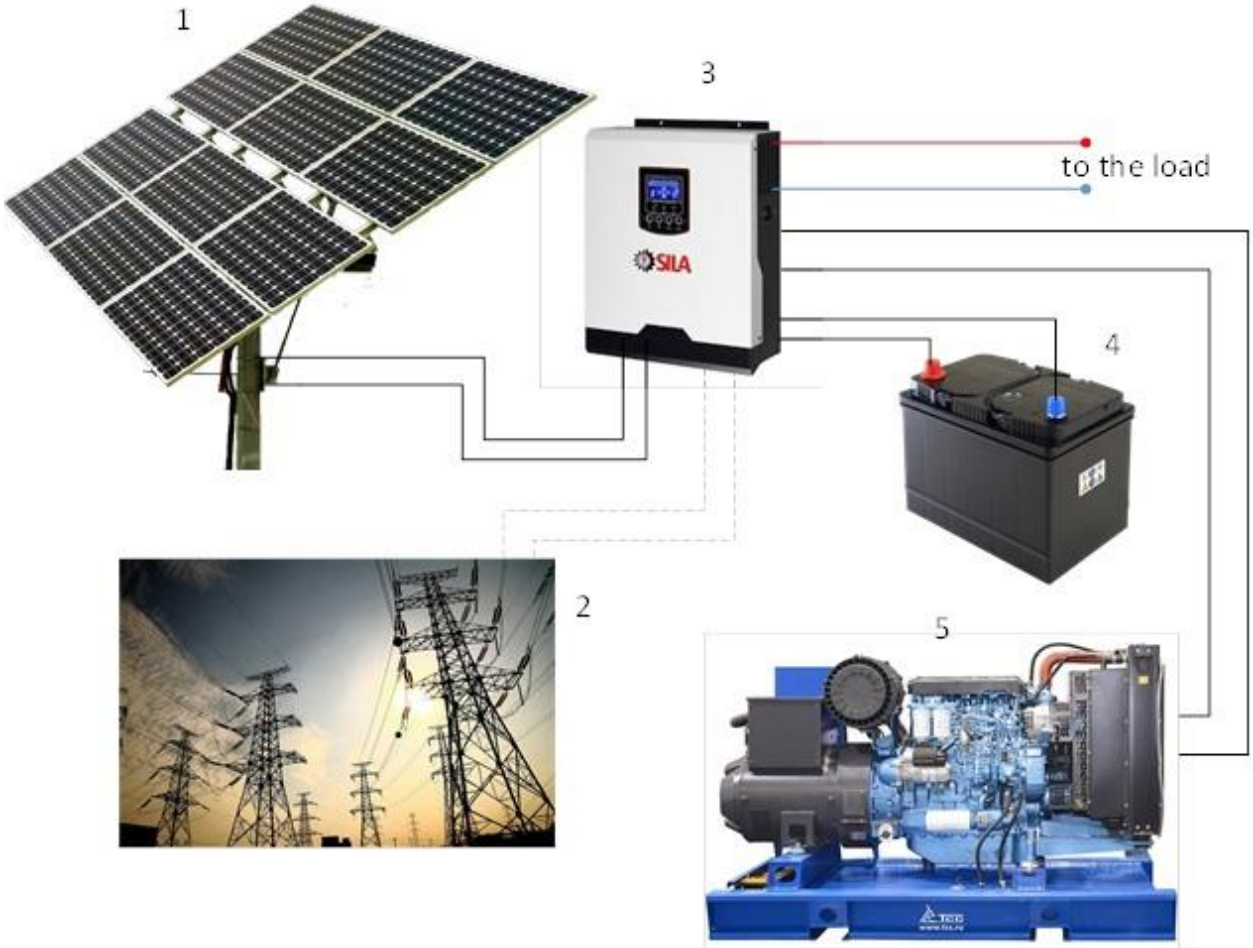

Figure 4.1 - Operating mode of the PVS. 1 - solar panel, 2 - city grid, 3 - power and charge controller, 4 - energy storage device, 5 - diesel generator

The basis of any photovoltaic installation is a solar panel. Currently, there are a huge number of types, categories, and manufacturers of batteries. Let's focus on some of them.

The domestic plant Hevel (Hevel) is engaged in the production of solar panels based on the heterojunction HJT. Such panels combine the advantages of both amorphous (thin-film) and time-tested crystalline technology. The cell efficiency can reach 22% and the temperature coefficient of power -0.28. The power range of the produced SBs ranges from 90 to 310 W.

Another domestic manufacturer - JSC "RZMKP" produces solar panels with a capacity of 63-330 W, with a maximum efficiency of 16.5% and temperature coefficient of power -0.427. A distinctive feature of the products of this manufacturer is automated production, which allows achieving high quality and purity of crystals in the cells of the panel.

Of foreign manufacturers, we can single out quite a popular one - Delta. The company specializes in the production of batteries, as well as solar modules. The main production is located in China. The range of output modules ranges from 15 to 320 watts. Thanks to a patented manufacturing technology of the module cells provide efficiency of the cell 19.2% and 16.5% of the module. The temperature power coefficient is -0.39.

One of the major companies manufacturing solar trackers for solar panels is Energy Track. Their trackers can be both single-axis and dual-axis, and allow you to track the position of the sun all day long.

The main features of Energy Track's solar trackers are:

- 0.1-degree accuracy;
- Turning time of 1s/degree or 0.16 revolutions per minute;
- Maximum wind speed of 50 meters per second;
- Peak wind velocity for collapsing the installation into a protective position is 12 meters per second;
- The installation discreteness is 1-10 degrees;
- Angle of elevation above the horizon is 0-80 degrees;
- Angle of azimuth position change 0-220 degrees;
- Operating temperature range -45 +50 degrees;
- Protection class IP67.

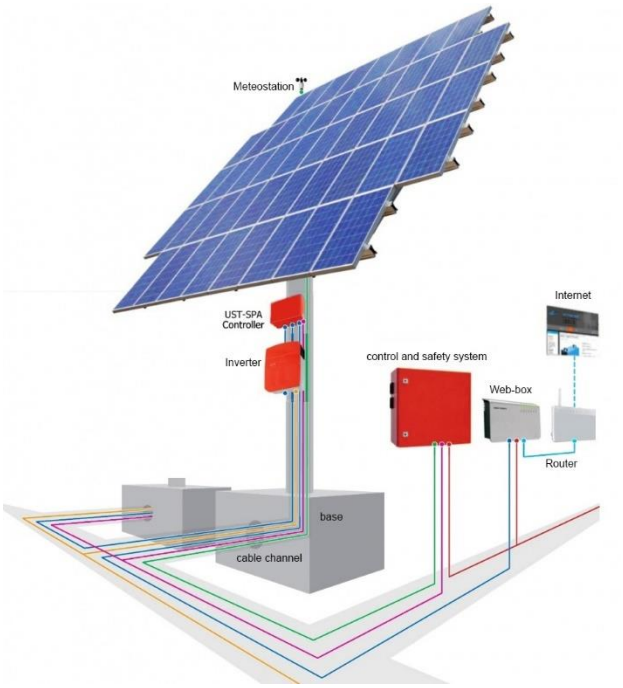

Figure 4.2 - Composition of the UST solar tracker [58]

Another manufacturer of solar trackers, United Solar Technologies, produces trackers of various models and configurations.

In general, the device consists of:

- A supporting structure consisting of a fixed and a moving part, the moving part has one or two axes of rotation (Figure 3.10);
- Orientation (positioning) system of the moving part of the tracker, consisting of actuators and their control device;
- Safety systems include lightning protection, overload protection, weather station designed to warn the system about hurricanes, hail, snow, ice, adverse weather conditions. By analyzing data from the weather station, the system reorients the tracker to a position where adverse factors will be minimized during their effect, and working surfaces are protected from damage or deterioration. It also includes stabilizers;
- A control system and interface designed to set up, monitor, and maintain the power system;
- Remote access system - for remote monitoring and control of the system;
- Navigation system - for determining the geographical position of the system, the altitude above sea level (for trackers on a mobile base). Navigation is not obligatory on stationary trackers. Setting values of latitude, longitude, altitude above sea level of the place, where the tracker is installed, are entered by the supplier during installation of the system.
- Inverter converts the DC voltage coming from the tracker payload (PV modules, etc.) into AC 220V (110V) and transmits it to the consumer or the receiving station, simultaneously powering the tracker. The number of inverters on the tracker can be from one to three. Inverters are made in a protected version (field) or in a housing to be installed in the room. Connection schemes of inverters in the system can be different.

The considered equipment is a modern achievement of science and industry in this field. Its use will help to test the model in conditions closer to the real one, as well as to check all the initial data.

4.2 Calculation of consumption loads and equipment selection

The main task when selecting equipment is to select the required number of devices. For this purpose, it is necessary to calculate loads of the power supply object, which is a country house (figure 4.3) with a certain list of equipment. For the comfortable living of a family of 4 people, a modern house has an area of about 150 m2 (Fig. 4.4). The calculation was done by the method of demand coefficient. Table 4.1 shows a summary of the number and characteristics of the equipment.

Heating in the house in question, as well as water supply (cold and hot) is central. This type is chosen because in Russia it is more profitable and reliable to heat the house with a centralized system. However, if we talk about autonomous systems for hot and cold water, the most rational solution would be a boiler heating. The boiler is heated with wood, coal or gas.

Figure 4.3 - Electricity supply object - country house

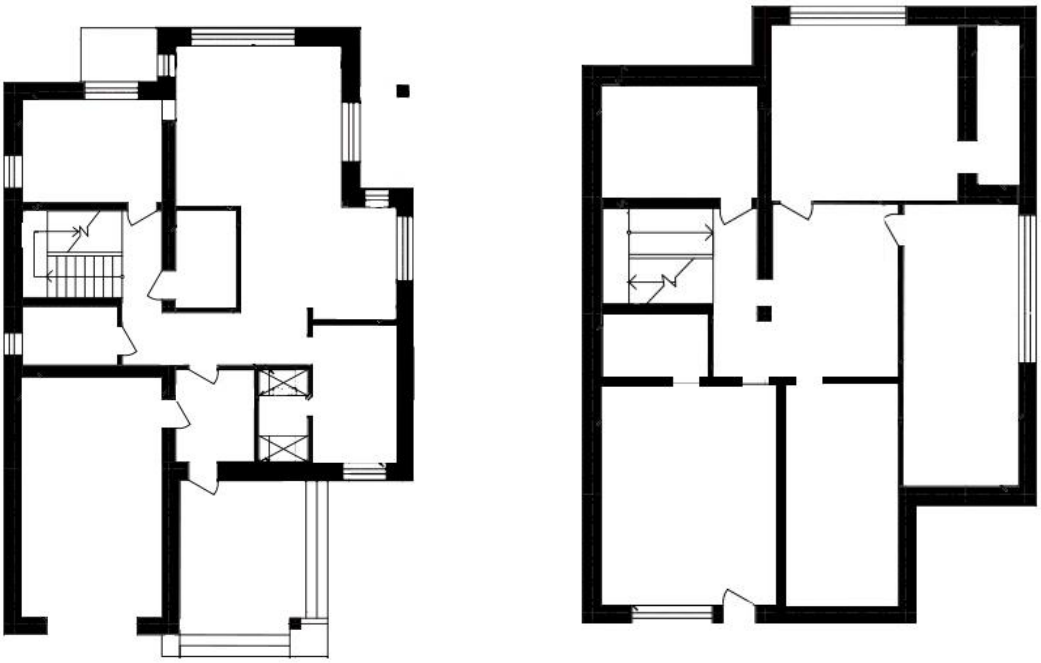

Figure 4.4 - House plan (1st and 2nd floor, respectively)

Table 4.1 - Data on electricity consumers

Room	**Electric devices**	**Rated (installed) power, kW**	**Kc**	**Rated power, kW**
Kitchen	Electric stove	9	0.2	1.80
	Dishwasher	2.2	0.1	0.22
	Refrigerator	0.6	1	0.60
	Kitchen Combine	4	0.1	0.40
	Electric kettle	2	0.3	0.60
	2 sockets 16A	7	0.1	0.7
	Electric light	0.144	0.2	0.03
Hall and corridors	2 sockets 16A	7	0.1	0.7
	Electric light	0.075	0.1	0.02
Bathroom	Fan	0.5	0.2	0.10
	Washing machine	2.2	0.3	0.66
	2 sockets 16A	7	0.1	0.7
	Electric light	0.045	0.2	0.02
Living Room	Air conditioner	2.2	0.2	0.44
	2 sockets 16A	7	0.1	0.7
	TV	0.08	0.1	0.01
	Electric light	0.144	0.2	0.03
Bedroom 1	Electric light	0.072	0.2	0.01
	2 sockets 16A	2.2	0.7	0.22
Bedroom 2	Electric light	0.072	0.2	0.01
	2 sockets 16A	2.2	0.7	0.22
Other	3 electric pumps	1.5	0.7	1.05
Total		44		7.86

Calculation example for air conditioner:

$$P_R = P_{nom} \cdot K_C = 2.2 \cdot 0.2 = 0.44\,(\text{kW}),$$

where Pnom - rated capacity of the electric device

Kc - demand factor (this is the ratio of the calculated power to the total nominal power of the group.).

Applying the chosen method of calculation, I got a contradiction: the total calculated load was less than the rated power of the most powerful electric receiver. This is a normal situation. In this case, I proceed

as follows: I equate the total load value to the power of the most powerful electric appliance, i.e. in my case, the electric stove. In other words, I obtain that the rated power of the cottage in question is 9 kW.

Moreover, I cannot rule out the theoretically possible case when all the appliances will be simultaneously included in the network. Then the load power will increase even more - practically to the total rated power of all electric consumers. To account for this variant, the following scheme will be implemented: photovoltaic panels will supply the calculated load - 9 kW. When the energy generated by them will not be enough (absence of the Sun or increase in the load), the automatics will connect a diesel generator.

Knowing the total design capacity, you can build daily load schedules. Applying typical load schedules for country houses [59], we obtain the following load schedules of the cottage in question by seasons (Figures 4.5-4.8).

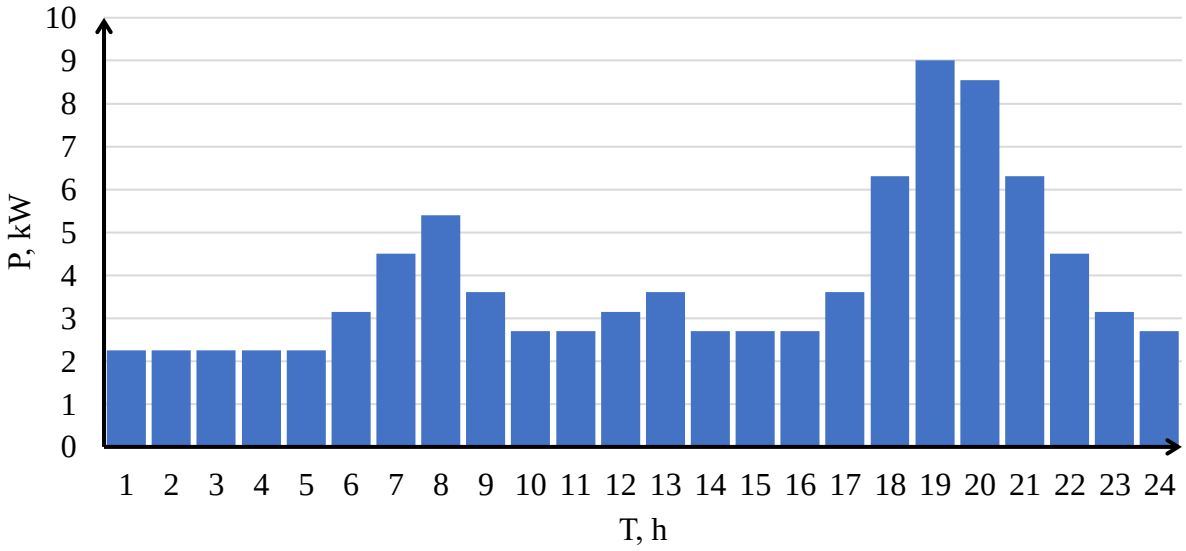

Figure 4.5 - Daily load schedule of the cottage in winter

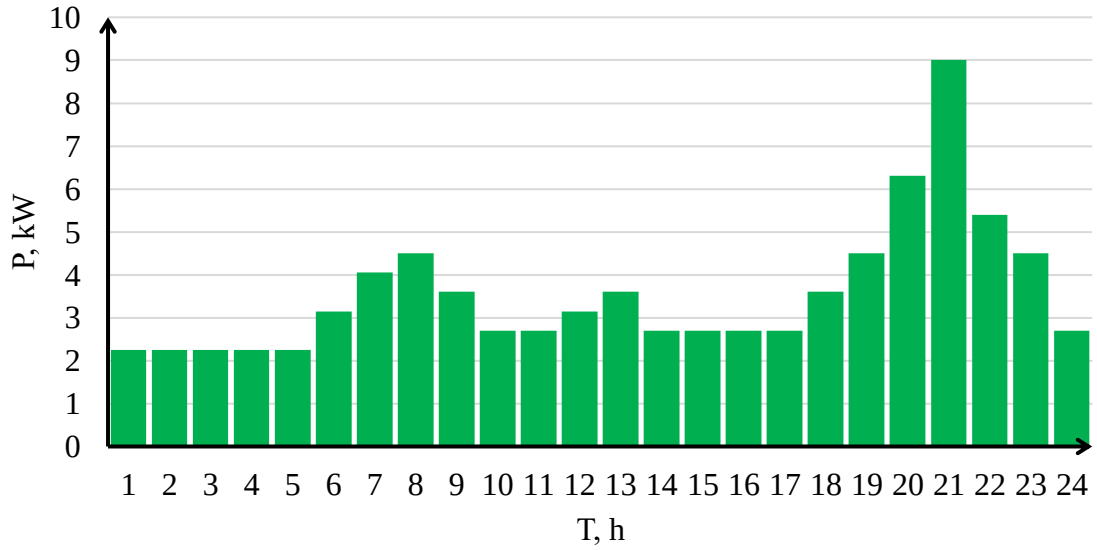

Figure 4.6 - Daily load schedule of the cottage in the spring period

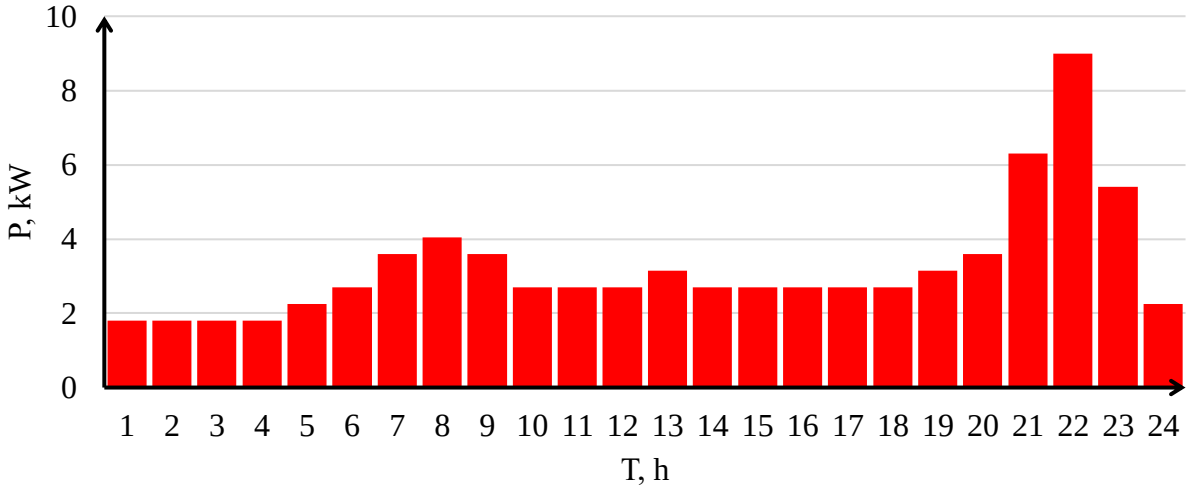

Figure 4.7 - Daily load schedule of the cottage in summer

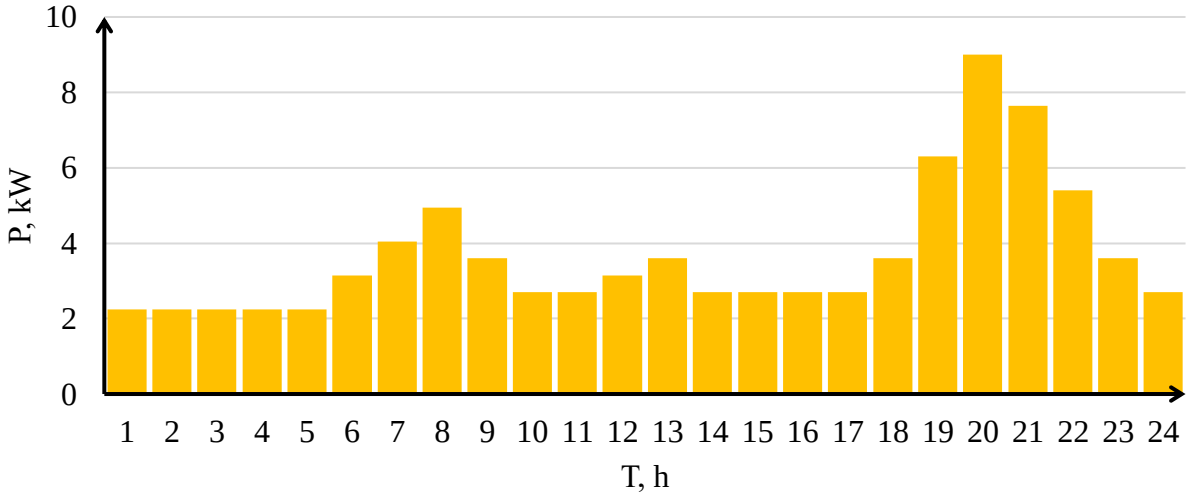

Figure 4.8 - Daily load schedule of the cottage in the fall

Next, it is necessary to calculate the amount of energy consumed for the year. To this end, it is necessary to determine the energy consumption every month, taking into account the seasonal coefficient kC [59].

Thus, in January, the total consumption will be:

$$W_{\text{january}} = W_{day} \cdot k_C \cdot n = 62.83 \cdot 1 \cdot 31 = 2859.75\,(\text{kW} \cdot h),$$

where Wday - the daily electricity consumption in the month in question, kWh,

kc - seasonality factor,

n - number of days in the month.

Calculations for other months are performed similarly. They are summarized in Table 4.2.

Table 4.2 - Annual electricity consumption

Month	k_C	**Number of days**	**Energy, kWh**
January	1	31	2859.75
February	1	28	2583.00
March	0.9	31	2385.45
April	0.8	30	2052.00
May	0.7	31	1855.35
June	0.7	30	1634.85
July	0.7	31	1689.35
August	0.7	31	1689.35
September	0.7	30	1852.20
October	0.8	31	2187.36
November	0.9	30	2381.40
December	1	31	2859.75
Total			26029.80

The graphical representation of the obtained values can be presented in the form of an annual load chart (Figure 4.9).

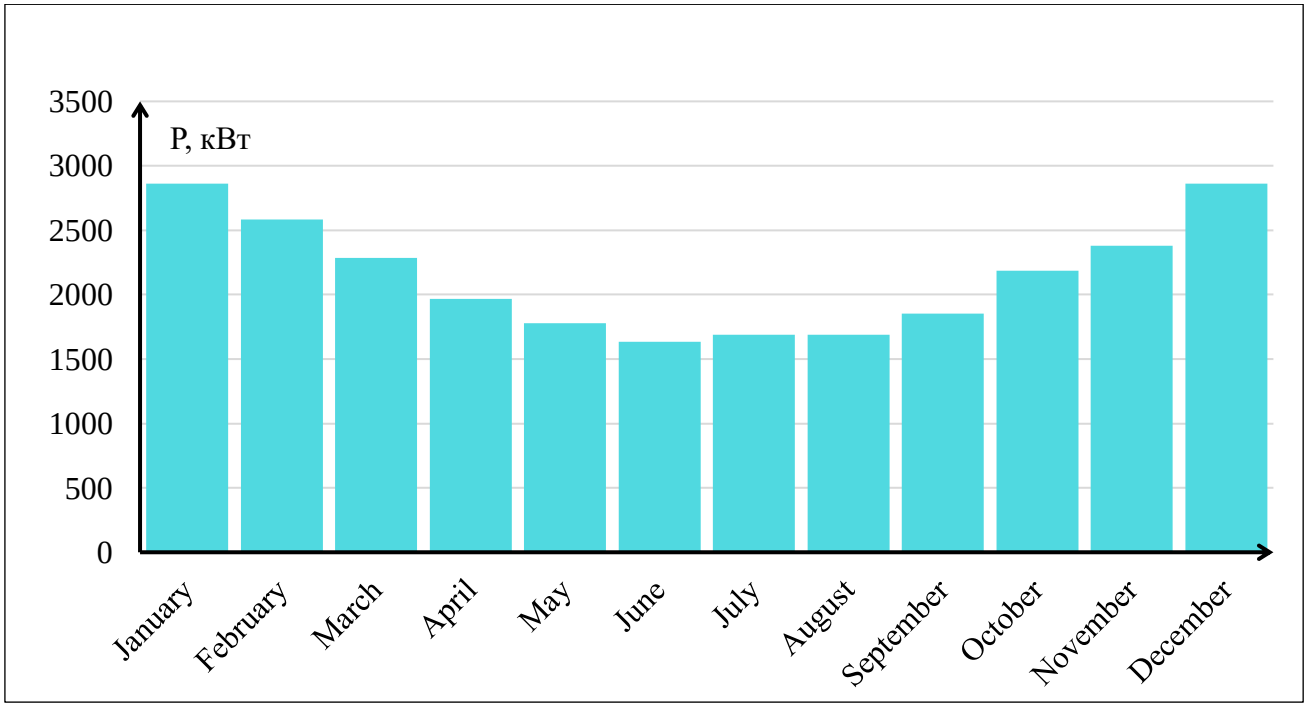

Figure 4.8 - Annual load schedule

To calculate the actual electricity production by the solar panels, the value of the average daily total solar radiation is used. To begin with, we will consider the variant without the tracker. So, for Alexandrovskoye village, the electricity generated per 1 m^2 per day:

$$W_{\text{gen. winter}} = \eta \cdot W_{\text{average winter}} = 0.18 \cdot 6.034 = 1.09\ (\text{kW} \cdot h/\text{m}^2),$$

where W average winter - the average total radiation during the winter period, kWh,

η - efficiency of the solar panel.

The area of solar panels required to cover loads of the generation is determined from the following ratio:

$$S_{required} = \frac{W_{con.\text{winter}}}{W_{gen.\text{winter}}} = \frac{92.25}{1.09} = 84.8\ (\text{m}^2),$$

where Wcon. winter - the daily electricity consumption of the cottage in winter, kWh.

Thus, knowing the parameters of the solar panel (Table 4.3) and the data on energy consumption/production, we obtain the following number of solar panels:

$$N = \frac{S_{required}}{S_{\text{panels}}} = \frac{84.8}{1.62} = 52.34 \approx 53\ (\text{units}).$$

Table 4.3 - Parameters of the solar panel SilaSolar 350W PERC (5BB) [60]

Type	Monocrystalline PERC
Power	350 W
Number of elements	72 units (6 x 12)
Cell size	156 x 156 mm
Off-load voltage	45.09 V
Operating voltage	37.58 V
Short circuit current	9.88 A
Operating current	9.32 A
Maximum voltage, V	1000
Module Efficiency, %	18.03
Cell efficiency, %	20.60
Cell Efficiency, %	at least 30 years
Service life	not more than 10%
Power loss in 12 years	not more than 20%
Power loss in 30 years	Anodized aluminum alloy
Frame material	Textured, tempered impact resistant
Front glass	A

Class	Up to 2400Pa (244 kg per square meter)
Wind Load	Up to 5400Pa (550 kg per square meter)
Snow load	Max. diameter 25mm, max. speed 83km/h
Graduation resistance	-40°C to +85°C
Operating Temperature	1956 mm
Length	992 mm
Width	45 mm
Height	1.62 m^2
Total Area	23 kg

The values of the generated energy for the other seasons and geographical points are calculated in the same way. The data are presented in Table 4.4.

Table 4.4 - Necessary number of panels for a stand-alone mode without tracker

Geographical object	Season	W_{con}, kW·h	W_{gen}, kW·h /m^2	$S_{required}$, m^2	N, units
Alexandrovskoe	Winter	57.4	0.36	257.11	159
	Spring	50.96	0.89	92.33	57
	Summer	48.44	1.07	72.81	45
	Autumn	54.88	0.62	142.62	89

The same values, but with the application of different types of a tracker, are defined further. The data is presented in the summary table 4.5.

Table 4.5 - Summary data on the number of panels with different types of tracker

Geographic object	Season	Without Tracker	With Slope Tracker	With Azimuth Tracker	With Slope and Azimuth Tracker
Alexandrovskoe	Winter	159	141	122	120
	Spring	57	48	31	40
	Summer	45	37	22	21
	Autumn	89	79	68	71

Since the PVS operates autonomously and the sun does not shine for all 24 hours a day, it is necessary to store the energy accumulated during the bright part of the day so that it can be used during the periods when there is no light. This is what batteries are for. Their role will be performed by lead-acid Delta GX 12-12 with the following technical characteristics:

Table 4.6 - Battery Specifications Delta GX 12-12 [61]

Rated voltage	12 V
Number of elements	6
Service life	15 years
Rated capacity (at 25°C)	
20 hourly discharge (0.6 A; 1.75 V/pel)	12 Ah
10-hourly discharge (1.07 A; 1.75 V/cell)	10,7 Ah
5-hourly discharge (1.94 A; 1.75 V/pel)	9.7 Ah
Self-discharge	3% capacity per month at 20°C
The internal resistance of a fully charged battery (25°C)	17.5 mOhm

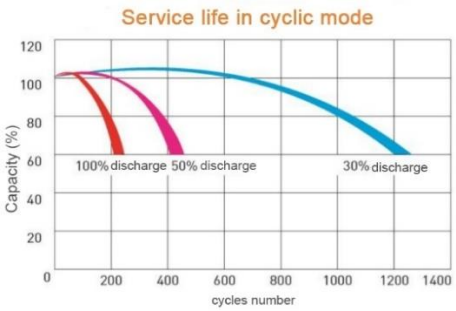

Figure 4.8 - Cycle life of the DELTA battery [61]

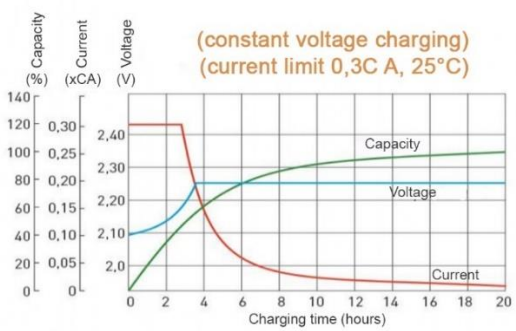

Figure 4.9 - Charging characteristics of the DELTA battery [61]

To determine the required number of batteries, as well as their depth of discharge, proceed as follows. First of all, the following conditions must be taken into account:

- The efficiency of the battery during charging - 90%;
- The efficiency of the battery during discharging - 90%;
- Maximum charging current - 0,2A;
- Depth of discharge - no more than 30%.

Since all the energy generated by the solar panels goes to maintain the charge of the battery, and already from the batteries of storage devices is fed to consumers, the maximum capacity of the battery in the winter months will be:

$$C_{ACB} = \frac{W_{gen.winter} + 0.2 \cdot W_{gen.winter}}{U_{ACB}},$$

where $W_{gen.winter}$ - generated electric power during the period under consideration, kW;

U_{ACB} - nominal battery voltage, V.

$$C_{ACB} = \frac{93.41 + 0.2 \cdot 93.41}{12} = 9.34\,(\text{kA} \cdot h).$$

Next, you need to determine what the capacity will be, taking into account the depth of discharge. So, for a depth of discharge of 30% the total capacity of the batteries will be:

$$C_{ACB(30)} = \frac{C_{ACB} \cdot 100\%}{30\%} = \frac{9.34 \cdot 100}{30} = 31.14\,(\text{k A} \cdot h),$$

and the number of batteries will be:

$$N_{ACH(30)} = \frac{C_{ACB(30)}}{C_{ACB(\text{nom})}} = \frac{31.14 \cdot 10^3}{200} \approx 156 \text{ (units).}$$

Similarly, the calculation of the number of batteries for other geographical points, seasons, and types of trackers is carried out. The calculation data is summarized in Table 4.7.

Кроме того, необходимо понимать, каким образом будет происходить зарядка-разрядка аккумуляторов в течение дня. С этой целью была построена циклограмма аккумуляторных батарей (figure 4.10) для периода 48 ч. Двадцатичетырехчасовой период не будет показательным, поскольку было принято, что первоначально АКБ была заряжена на 100 %.

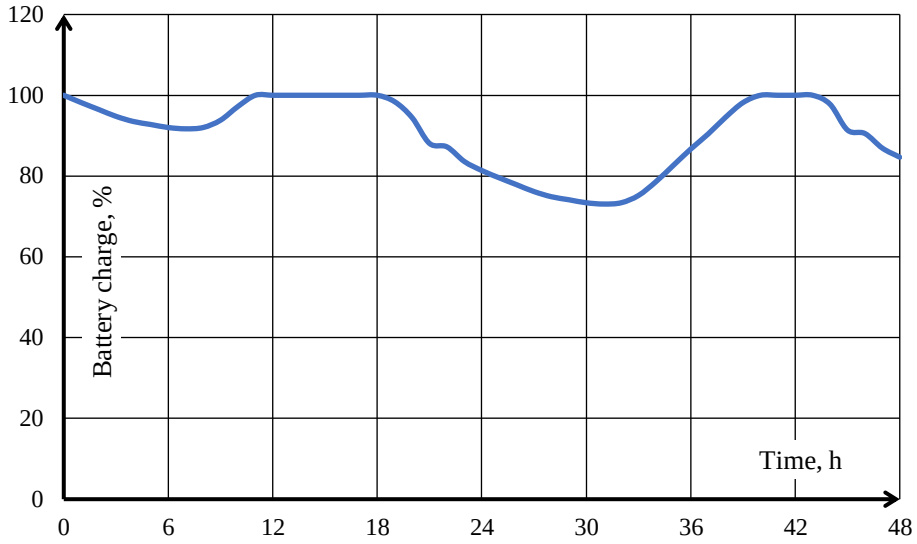

Figure 4.10 – Циклограмма аккумуляторной батареи

Построенная циклограмма позволяет визуально определить глубину разряда АКБ в интересующий момент времени, а также оценить, в какой период необходимо ограничивать зарядный ток, а в какой ограничивать ток разряда.

It is not possible to change the number of panels and batteries depending on the time of year. Therefore, it is accepted to install the "worst" option - the maximum number of panels in winter to cover the load, and the corresponding number of batteries.

Table 4.7 - Summary data on the number of batteries for different tracker types

Geographic object	**Season**	**Without Tracker**	**With Slope Tracker**	**With Azimuth Tracker**	**With Slope and Azimuth Tracker**
Alexandrovskoe	Winter	154	131	97	91
	Spring	137	118	90	88
	Summer	130	120	84	83
	Autumn	149	125	90	89

To ensure the quality of electricity requires a charge controller and inverter, which converts the DC voltage into alternating sinusoidal, and allows you to charge the battery. The projected PVS uses a SILA-M 20kW inverter system with the following features:

- Pure sine wave output
- Microprocessor control
- Built-in charge controller
- Several operating modes: parallel to mains, autonomous, parallel to mains in standby mode
- Large LCD shows all basic information about the solar power system operation
- Possibility of connection with computer to set and monitor the operation of a power supply system
- Adjustment of charging current
- Setting the lower and upper threshold for charging batteries
- Output for controlling external devices (such as generators)

and the following technical parameters (Table 4.8):

Table 4.8 - Parameters of the SILA-M 20kW inverter system [62]

Output waveform	Pure Sine
Built-in charge controller	MPPT
Output Voltage	230B +-5%
Frequency	50 Hz
EFFICIENCY	93%
Overload protection	110-150% - 10 sec; >150% - 5 sec
Peak power	40 000 W < 5 sec)
DC rated input voltage	48 V
Own consumption	5 A / 250 W
Maximum solar panel power	15 000 W
Charging current	50 - 300 A (programmable)
Rated battery voltage	48 V
Lower and upper battery voltage thresholds	programmable
The maximum voltage of solar panels	145 V (per inverter)
Working voltage range of solar cells	60~115 V (per inverter)
Storage Temperature, °C	-15˚C to +60˚C
Operating temperature, C	0°C to -55˚
Humidity	20~90%
Dimensions, mm	120 x 295 x 468 (each inverter)
Net Weight, kg	70

Since the inverter has a built-in charge controller function, this device is not required separately. Now let's consider the mains mode. The most rational and efficient scheme would be the one when during daylight hours, when solar radiation is present, the load is powered by the PVPP, and at other times, when the sun is not present, the consumer receives power from the city power grid. In this mode of operation, there is no need for energy storage - the power grid itself plays its role. The previously selected inverter is also suitable, as it can operate in this mode. Let's recalculate the number of panels.

From the calculations created by the model I have got that in the village Alexandrovskoye Sun is active: in winter from 7 to 16 hours, in spring from 6 to 20 hours, in summer from 5 to 22 hours, in autumn from 6 to 17 hours. Thus, the area of solar panels required to cover the loads of the generation is determined from the following ratio:

$$S_{required} = \frac{W_{con.winter'}}{W_{gen.winter}} = \frac{36.9}{1.09} = 33.92\ (\text{m}^2),$$

where Wcon.winter' - the daily electricity consumption of the cottage in winter from 6 to 16 hours, kWh.

Thus, the number of solar panels (Table 4.9):

$$N = \frac{S_{required}}{S_{panels}} = \frac{33.92}{1.62} = 21\ (\text{units}).$$

Table 4.9 - Summary of the number of panels with different types of trackers in network mode

Geographic object	**Season**	**Without Tracker**	**With Slope Tracker**	**With Azimuth Tracker**	**With Slope and Azimuth Tracker**
Alexandrovskoe	Winter	59	56	53	53
	Spring	37	36	28	26
	Summer	37	34	28	24
	Autumn	39	35	32	31

According to [63] for apartment buildings the allocated maximum power of single-phase load is 5,5 kW, for a private house - 15 kW. Returning to p.p. 4.2, Table 4.2, it should be noted that in the considered case of inclusion of all electrical consumers in the network, let's assume that to ensure reliable redundancy load power is equal to the standard-provided - 15 kW. The choice of the diesel generator is made by the total design load power.

In this case the model "EUROPOWER EPS193DE diesel generator" for 15,2 kW is suitable (Figure 4.11):

Figure 4.11 - Diesel generator EUROPOWER EPS193DE

Thus, in general, the functional scheme of the PVS in Alexandrovskoye will look as follows:

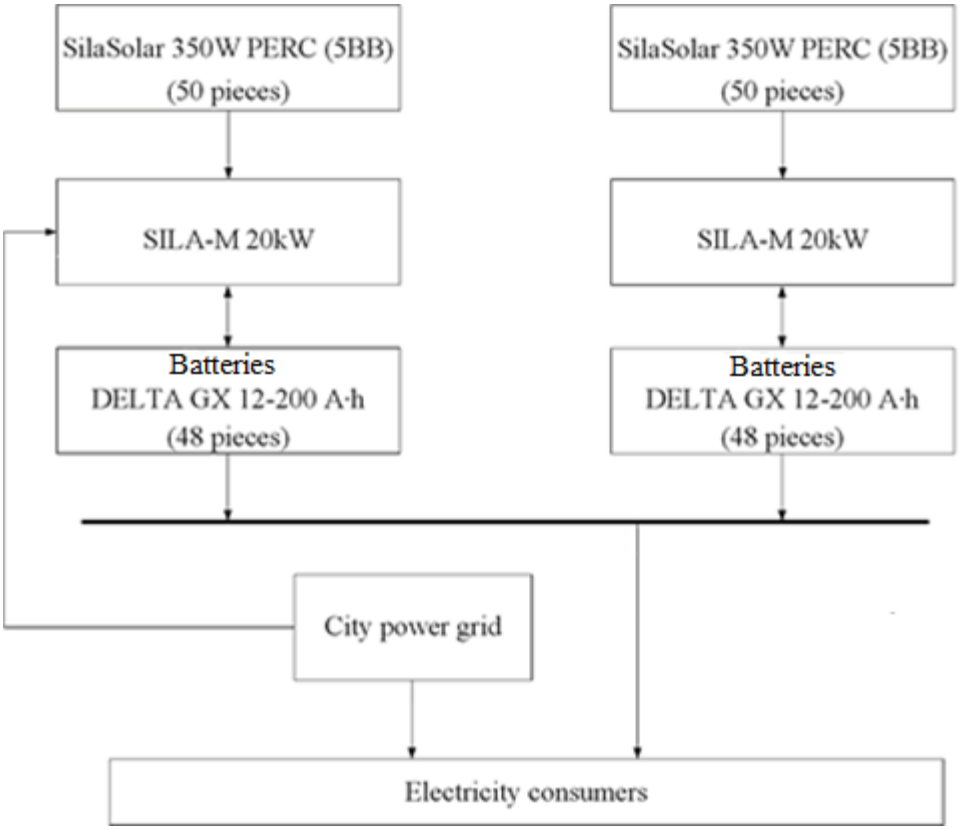

Figure 4.12 - Functional diagram of the PVS in the network mode

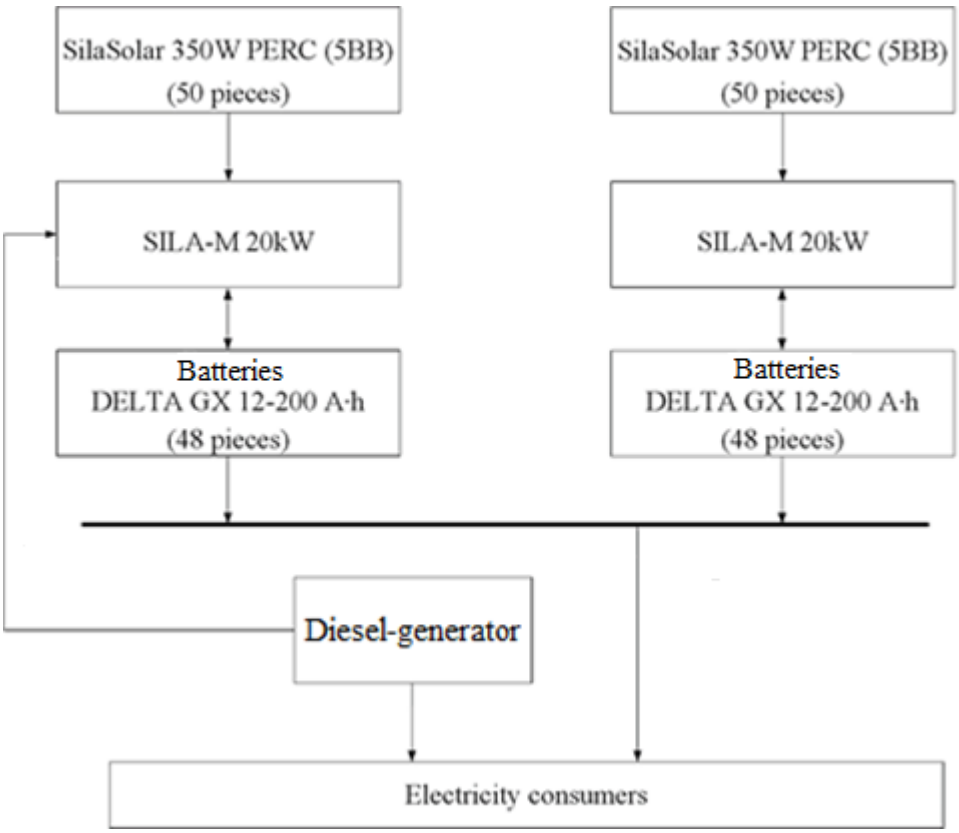

Figure 4.13 - Functional diagram of PVS in stand-alone mode with a diesel generator

4.3 Overview of ready-made tracking solutions

There are many ready-made solar tracker solutions on the market. They are presented both in the catalogs of large, established manufacturers, such as UST and in the lower price range. A prime example of such a group of manufacturers is the trading platform Alibaba.com. It offers a wide range of tracking systems. Let's look at some of them.

Figure 4.13 - Hua Yue Tracker [63]

One of the representatives of trackers with two positioning axes is the tracker of the company Hua Yue [63]. Its characteristics are presented in Table 4.11.

Table 4.11 - Hua Yue Tracker Characteristics

Project	With two axes tracker
Controller type	MCU
Control core	MCU (32bit)
Control algorithm	Astronomical algorithm + Closed loop position sensor
Protocol	RS485
Wind protection	У
Night Return Mode	У
A reverse direction tracking algorithm	У
Inverter intelligent tracking	Adaptable to customer requirements
Protection level	IP66
Anemometer	У
Communication network type	Bluetooth (WIFI, 4G can be configured)
Communication network mode	RS485
GPS	У
Heavy rain cleaning mode	Optional
Snowplow mode	Optional
Rotation position Protection mode	Sensor protection + Software protection
Drive unit	Rotary actuator + 1 * linear actuator (optional)
Drive protection	У
Tracking accuracy (°)	≤ 1 °
System power supply	L + N (two-phase input) 100V ~ 240VAC (wide input voltage range)
	(PV cord can be configured to receive power from 1000V to 1500V, lithium battery backup)
Power supply	Stand alone/external power supply

System voltage	DC24
Drive power (W)	350W
Tracking range azimuth (°)	-120° ~ + 120° / -135° ~ + 135° (adjustable)
Tracking Range Altitude (°)	0 ~ 60 °
Warranty	The whole machine 3 years (excluding mechanical design, damage, and force majeure factors)
Operating Temperature (℃)	Standard default configuration-30 ℃ ~ + 70 ℃ special setting

Another typical solution from the Alibaba site is a two-axis tracker from Wanda [64], shown in Figure 4.12. Its distinctive feature is two motors: a linear servo-drive is used to correct the panel angle of inclination, and a hydraulic motor is used to rotate azimuth.

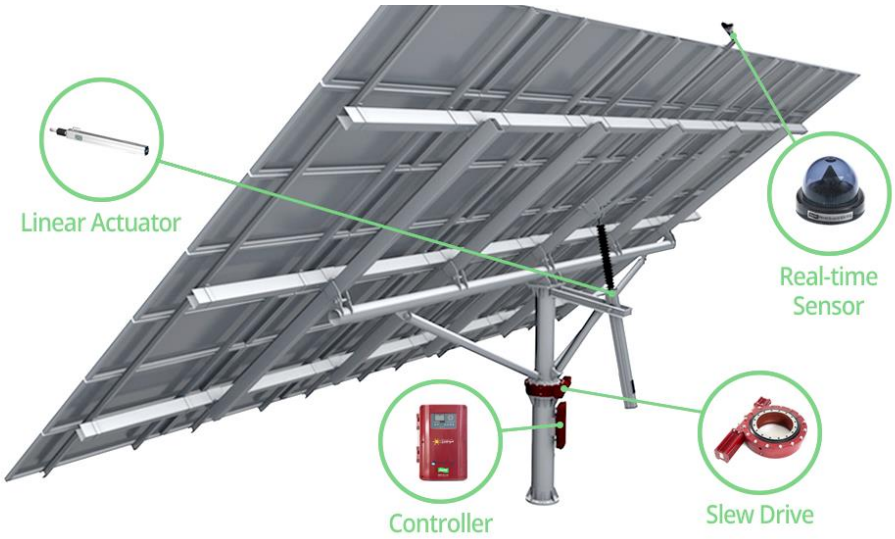

Figure 4.14 - Wanda Tracker [63]

Thus, Alibaba has a huge number of solar trackers at different price points, as well as different characteristics.

4.4 The final result of chapter 4

The annual consumption of electric power of the selected power supply object - a country house - is 16031,46 kWh. Two modes of operation of the PVS were considered: stand-alone and grid. In each mode of operation the following equipment was determined in number:

Table 4.10 - Quantity of PVS equipment at different modes of operation

	Number of panels, units				Number of batteries, units			
	without tracker	angle tracker	azimuth tracker	two-axis tracker	without tracker	angle tracker	azimuth tracker	two-axis tracker
	Stand-alone mode of operation							
Alexandrovskoye	99	152	144	143	154	155	97	154
	Network mode							
Alexandrovskoye	59	56	53	53	-	-	-	-

Thus, the smallest number of panels is observed when the azimuth tracker or the azimuth and tilt tracker is used. However, with a reduction in the number of panels and the use of the tracker, energy production increases, which leads to an increase in the capacity and the number of batteries.

From a technical point of view, the use of a tracker is justified, expedient and profitable, but to see the full picture, it is necessary to make an economic comparison of modes of operation and types of trackers used.

5. Inputs for economic model

In this chapter the economic analysis and comparison of two modes of operation of the photovoltaic system will be made: stand-alone and grid-tied.

5.1 Investments

The initial investment is the purchase of equipment for PV-system. The investments are presented in Table 5.1.

Table 5.1. – Cost of equipment

type of equipment	**Costs prices include VAT, ₽**
Solar pannel HEVEL HJT-310 (310 W)	15 590.00 ₽
Fasteners for panels	27 660.00 ₽
Invertors system SILA-M 20kW	271 200.00 ₽
Controller DOMINATOR-MPPT-200-100	87 000.00 ₽
Battery Delta GX 12-200 (200 Ah)	48 497.00 ₽
Tracker UST-VSAT	1 100 000.00 ₽
Tracker UST-AADAT	1 450 000.00 ₽

Table 5.2 also shows the correspondence of the amount of equipment to the operating mode of the plant.

Table 5.2. – The amount of equipment and its cost for different modes of operation

	Initial investment (stand-alone mode)				**Initial investment (grid mode)**			
type of equipment	**no tracker**	**tilt tracker**	**azimuth tracker**	**tilt&azimuth tracker**	**no tracker**	**tilt tracker**	**azimuth tracker**	**tilt&azimuth tracker**
Solar pannel HEVEL HJT-310 (310 W)	159	159	144	143	58	58	53	53
Fasteners for panels	10	10	10	10	5	5	5	5
Invertors system SILA-M 20kW	1	1	1	1	1	1	1	1
Controller DOMINATOR-MPPT-200-100	2	2	2	2	2	2	2	2
Battery Delta GX 12-200 (200 Ah)	155	155	155	155	0	0	0	0
Tracker UST-VSAT	0	2	2	0	0	1	1	0
Tracker UST-AADAT	0	0	0	2	0	0	0	1
Total	**10 717 645 ₽**	**12 917 645 ₽**	**12 683 795 ₽**	**13 368 205 ₽**	**1 487 720 ₽**	**2 587 720 ₽**	**2 509 770 ₽**	**2 859 770 ₽**

In addition, in the grid mode of operation, the investment will be the annual payments for electricity provided by the central grid. In 2022, the cost per kWh of electricity is 2.39 ₽.

Table 5.3 shows the calculation of annual monthly electricity consumption.

The volume of electricity consumed from the grid was taken into account the fact that there is no sun in the sky in the Alexandrovskoye village from 24 to 6 and from 22 to 24 hours. Consequently, the load schedule must be covered by electricity from the grid. To determine the necessary amount of electricity consumption, we need to sum the consumption during these periods (previously presented load schedules by season). Thus, for winter, the daily demand for grid electricity is as follows:

$$2.25 \cdot 5+3.15+4.5+3.15+2.7=31.05 \text{ kW*h}$$

Next, you need to calculate the monthly demand for grid electricity for each month of the year. For example, for January we get:

$$31.5 \cdot 31=1046.25 \text{ kW*h}$$

Calculations for the remaining months, as well as the total annual consumption of grid electricity are presented in Table 5.3.

Table 5.3 – Calculation of electricity consumption per year

Month	Energy from network, kWh
January	1 046.25
February	945.00
March	1 632.15
April	1 579.50
May	1 632.15
June	1 890.00
July	1 953.00
August	1 953.00
September	1 161.00
October	1 199.70
November	1 161.00
December	1 046.25
Total	**17 199.00**

Thus, the annual payment for electricity will be 17199·2.39=46953 ₽.

5.2 Discount rate

The discount rate is the interest rate used to convert future cash flows into present value. The discount rate is used in determining the discounted value of future cash flows [67]. The discount rate takes into account the time value of money as well as the risk or uncertainty of future cash flows. For this project (a low-risk project), I take the discount rate as the risk-free rate of Russian government bonds. The discount rate is 10.57% [68].

5.3 Escalation factor

The escalation coefficient is the increase in tariff rates for goods as their degree of processing increases.

This paper considers escalation factors for equipment (0.04) and for electricity charges (0.078).

They were determined by the change in the price of the equipment and, accordingly, the change in the price of electricity. Thus, the escalation factor for Battery Delta GX 12-200 (200 Ah) batteries will

$$\mathrm{Ef} = \frac{(\cos t_{2022} - \cos t_{2018})}{\cos t_{2018}} = \frac{48497 - 46627}{46627} = 0.04.$$

5.4 Covering of payment by credit

Based on the fact that the cost of the equipment is determined by several million rubles, it was decided to cover half of the cost with a loan.

Due to the unstable economic situation in the world, the interest rate of the loan is too high. In this work, it was assumed that in a year the situation will stabilize and the interest rate can be reduced to a sane rate.

At the moment, the average interest rate in banks in Russia is 20%. This rate was taken for the first year of operation of the plant. For subsequent years, it was assumed that the interest rate would decrease to acceptable values - 10% - and the loan would be refinanced.

5.5 Maintenance cost

Among other things, it is necessary to consider the cost of equipment maintenance (solar panels, batteries, etc.).

As a rule, maintenance is 1% of the total cost of the equipment.

6. Financial analysis

The main task is not only to assess the economic benefits of each option, but also to determine the investment needed to implement each alternative.

The evaluation of the effectiveness of investments in projects usually focuses on the evaluation of such an indicator as the net present value (NPV).

6.1 Net Present Value

Net present value is the difference between the sum of discounted cash flows and the cost of the project. The NPV equation is according to [69] and is:

$$NPV = \sum_{t=0}^{n} \frac{CF_t}{(1+r_i)^t} = \sum_{t=1}^{n} \frac{CF_t}{(1+r_i)^t} - INV,$$

where CF_t is Cash flow in time period *t*;

r_i is Discount rate;

INV is Investment;

n is the number of periods;

t is time period.

The criterion for project approval is a positive NPV value. If there are two or more possible projects to choose from, the project with the higher net present value is preferred.

Since the NPV calculation is based only on costs, the NPV for all alternatives considered will be negative, and the higher NPV will represent the better alternative. I will use the same economic model to calculate each project alternative.

6.2 Economic model calculation of Net Present Value

The previous sections provide all of the necessary data for the economic analysis. The next step is to calculate the NPV for each alternative. The results of the economic analysis are presented in Table 6.1.

Table 6.1. Economic calculation NPV

	no tracker	tilt tracker	azimuth tracker	tilt&azimuth tracker
stand-alone mode	-15 427 053,72 ₽	-17 895 955,16 ₽	-17 596 185,10 ₽	-18 361 759,97 ₽
network mode	-2 831 846,67 ₽	-4 066 297,39 ₽	-3 966 374,04 ₽	-4 359 153,81 ₽

I compared the alternatives according to the NPV calculations (figure 6.1) and chose the highest one. I can conclude that the network mode and without the tracker is the best.

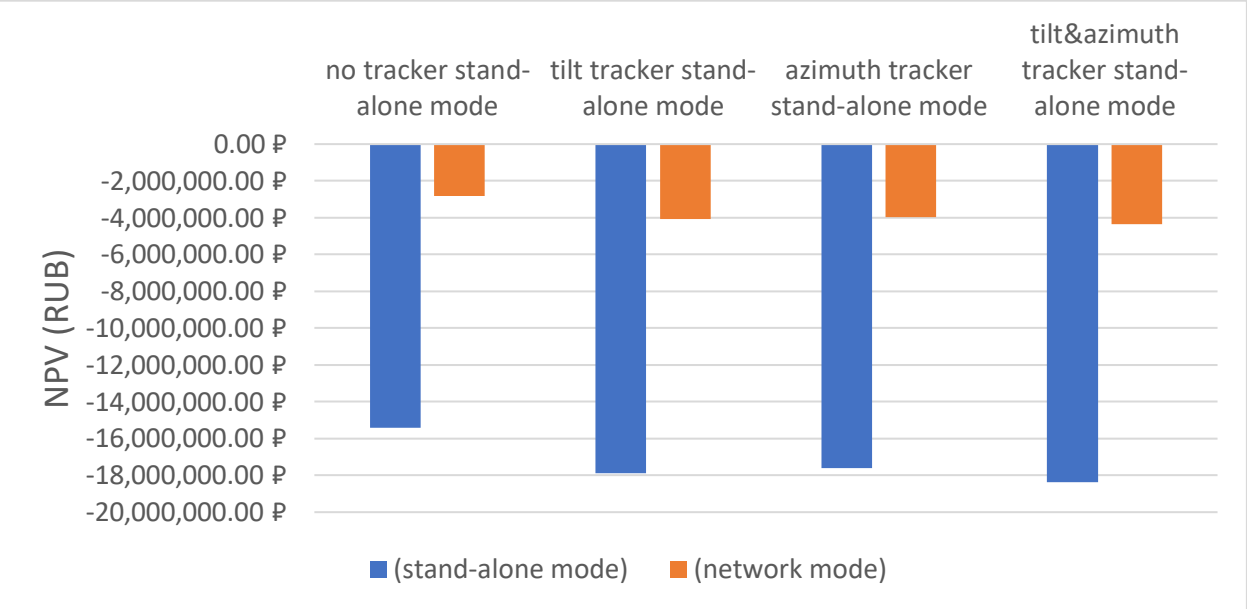

Figure 6.1 –NPV comparison

The result is logical, however, I should not forget that this is only an economic analysis, which does not give a complete picture. If I consider together the technical calculation presented in the previous chapters and the economic calculation from this chapter, we can conclude that the most advantageous would be: in stand-alone mode - azimuthal tracker, in network mode - also azimuthal tracker.

If you have to choose between these two modes, then, of course, the most expedient option would be the network mode. And this is also a logical option, because renewable energy is only economically viable where there is no central power supply.

6.3 Sensitivity analysis

Sensitivity analysis is a method of determining the effect of input independent parameters on the dependent variable. Sensitivity analysis is important when planning a long-term project. Some parameters may change significantly over the life of the project. Therefore, it is necessary to evaluate these changes and determine their impact on the profitability of the project.

I perform sensitivity analysis using a tornado diagram for the stand-alone mode with azimuth tracker, when the input parameters change by 10%. The tornado diagrams are shown in Figure 6.2.

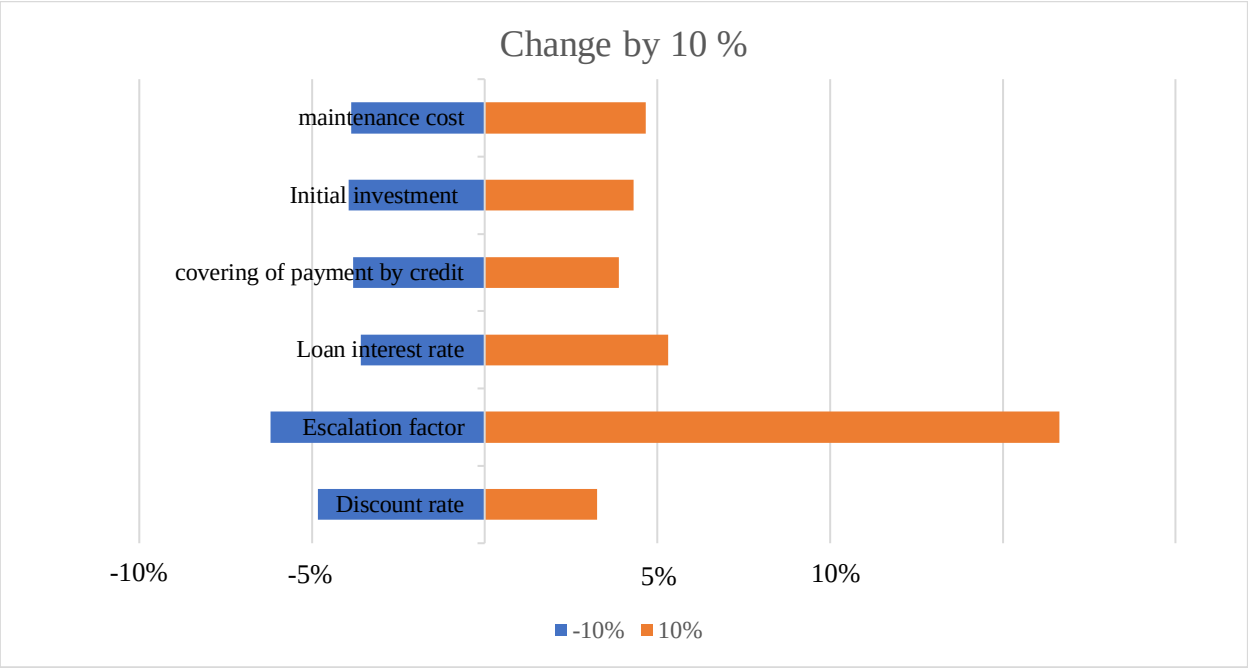

Figure 6.2 – The tornado diagram

It can be seen that the change in NPV is most strongly influenced by such parameters as the discount rate, the escalation factor and the loan interest rate. Sensitivity analysis is conducted for these parameters.

Let us consider the effect of a change in the discount rate on NPV for each alternative. The dependence of NPV on the discount rate is shown in Figure 6.3, 6.4. The value of the discount rate changes by 10%, either positively or negatively. As the discount rate increases, the NPV increases. However, changing the discount rate does not affect the decision. For all alternatives, NPV increases proportionately. The shape of the curve is explained by negative cash flows.

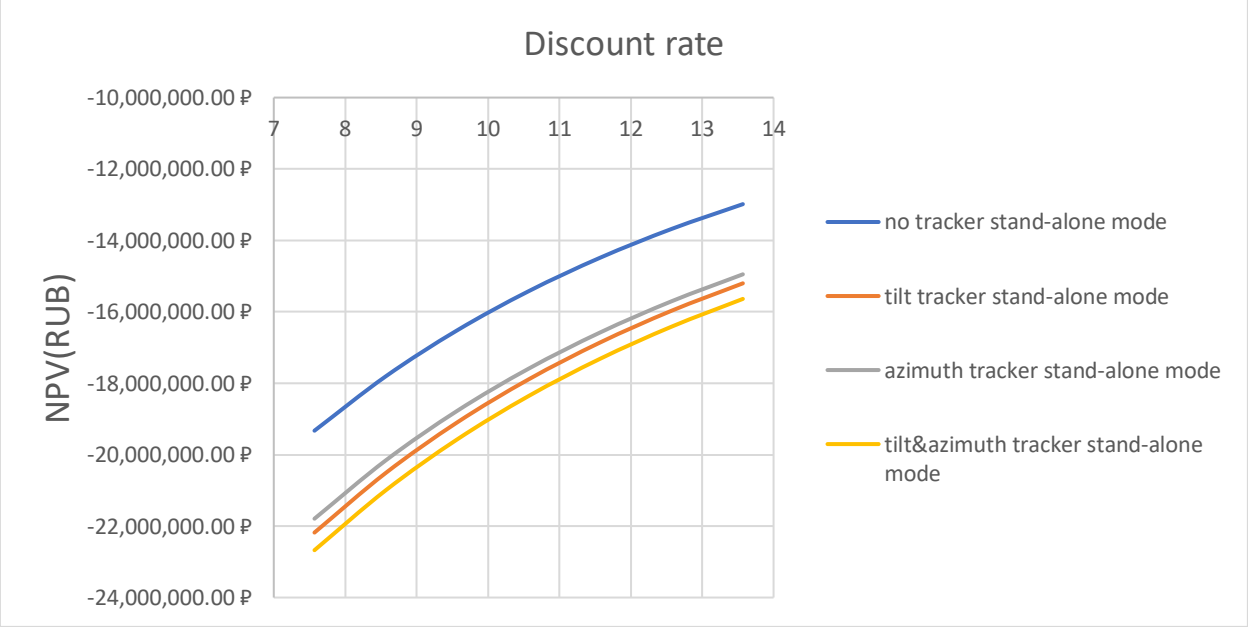

Figure 6.3 – The dependence of NPV on the discount rate (stand-along mode)

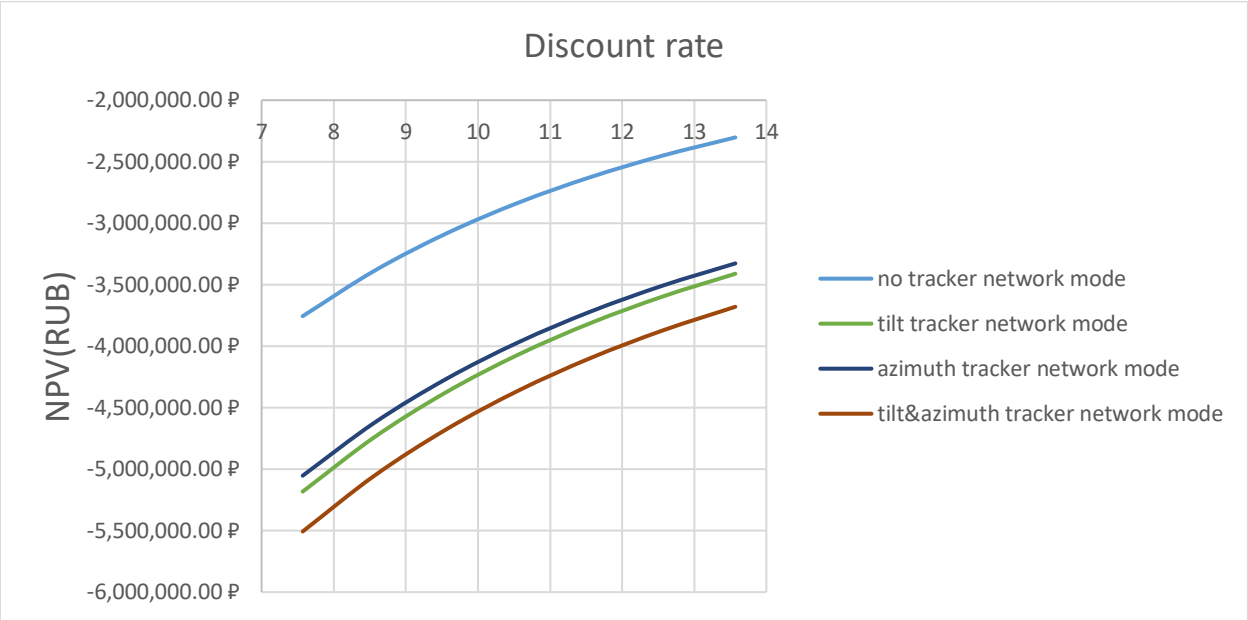

Figure 6.4 – The dependence of NPV on the discount rate (grid mode)

Let us consider the effect of changes in the escalation factor on NPV for each alternative. The dependence of NPV on escalation factor is shown in Figure 6.5, 6.6. The value of the escalation factor changes by 10%, either positively or negatively. As the escalation factor increases, the NPV decreases. However, the change in escalation factor does not affect the decision. For all alternatives, NPV decreases proportionally. The shape of the curve is explained by the negative cash flows.

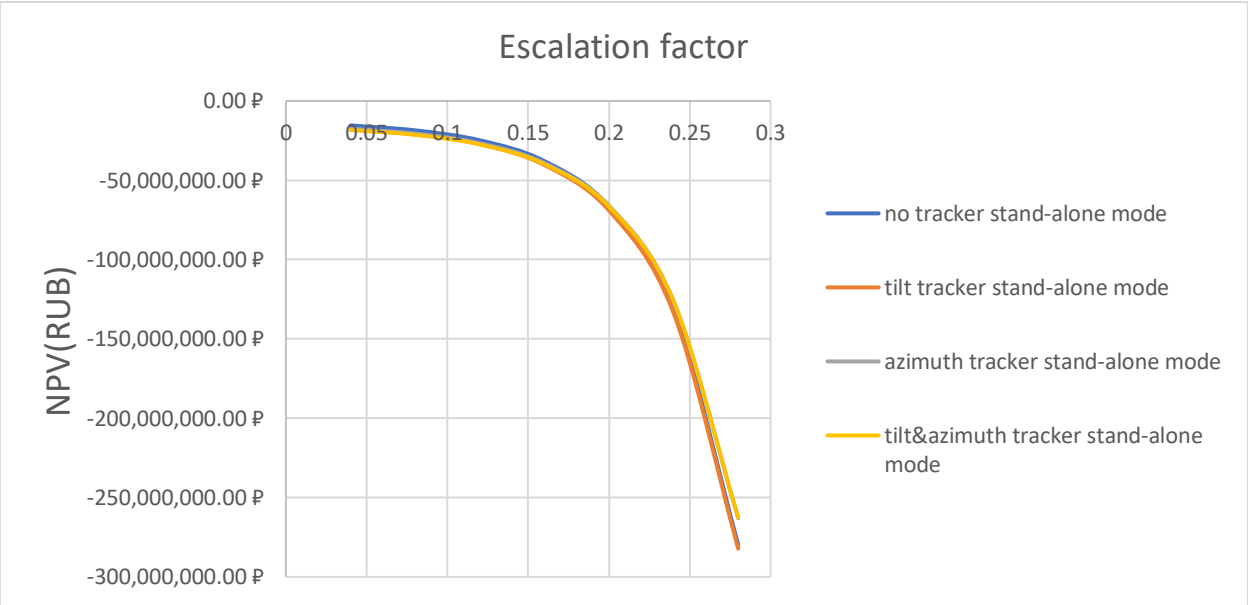

Figure 6.5 – The dependence of NPV on the covering of payment by credit (stand-along mode)

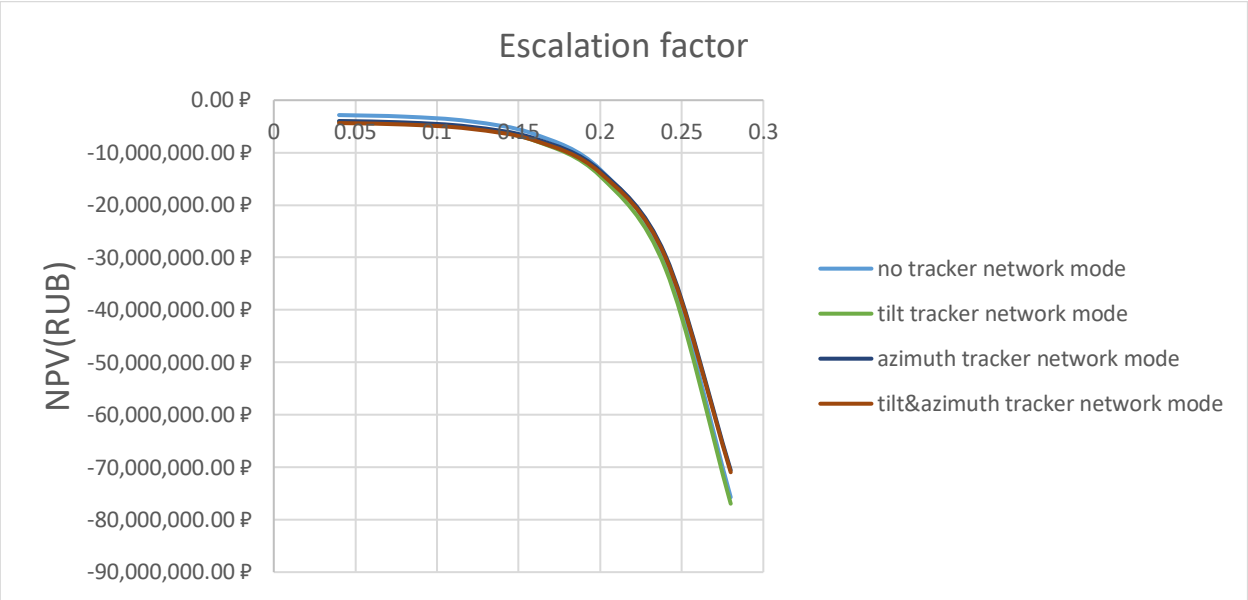

Figure 6.6 – The dependence of NPV on the covering of payment by credit (grid mode)

Let consider the impact of changing the loan interest rate on the NPV for each alternative. The dependence of NPV on the loan interest rate is presented in Figure 6.7, 6.8. The value of the loan interest rate varies by 10%, either positively or negatively. Because the loan interest rate, the NPV decreases. However, changing the initial investment has no impact on the decision. For all alternatives, the NPV increases proportionally. The curve form is explained by the negative cash flows.

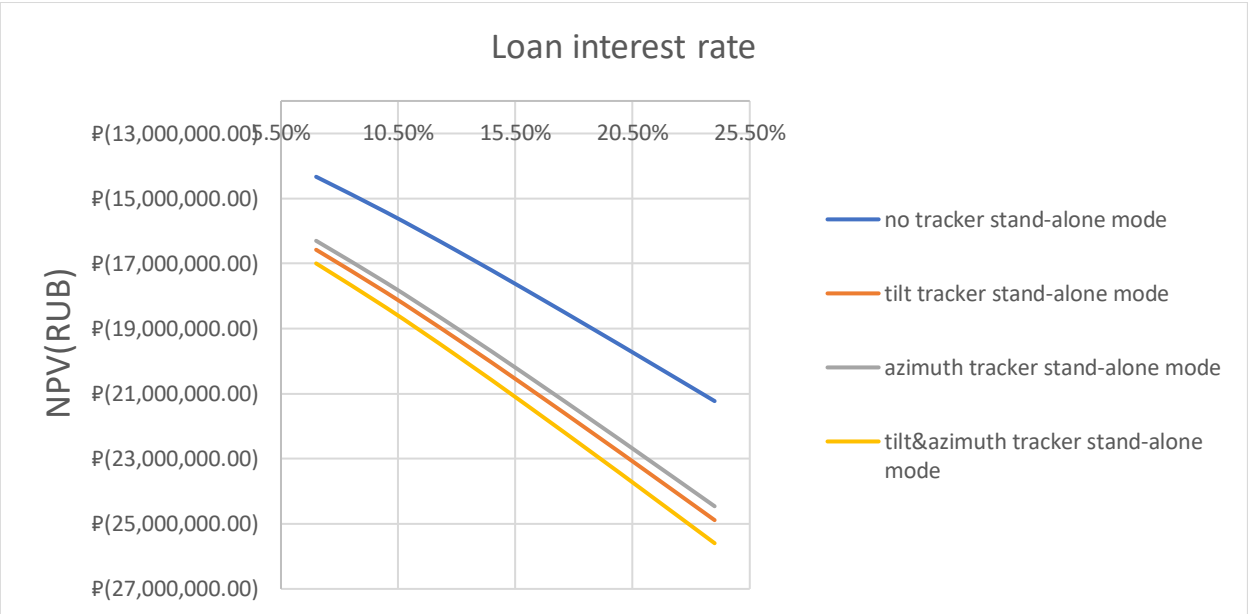

Figure 6.7 – The dependence of NPV on the initial investment (stand-along mode)

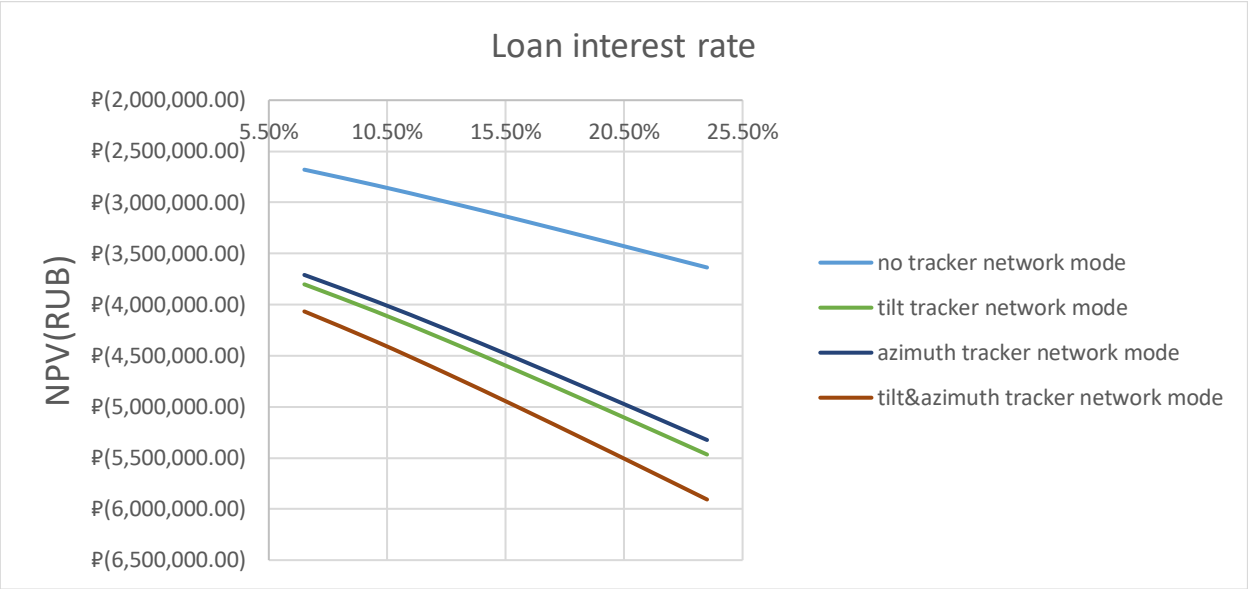

Figure 6.8 – The dependence of NPV on the initial investment (grid mode)

Conclusion

In this paper, a comparative analysis of the effectiveness of solar trackers in photovoltaic installations for electricity generation was made. The technical and economic components of the effectiveness of the implementation of the tracking system were considered.

There is an extensive world practice of using different types and kinds of solar trackers. Research on the effectiveness of their use has been conducted for several decades. Trackers can be uniaxial and biaxial, electrically driven or based on fluid expansion properties when heated. At the moment, the most promising ones are single-axis ones: a tracker that tracks the height of the Sun above the horizon, a tracker that tracks the azimuthal angle of the Sun, and a two-axis one: a combination of these two devices.

As part of the work under consideration, we developed a model of the arrival of solar radiation, the distinctive feature of which is the accuracy of insolation calculation - the error of 0.8-8.8%, depending on location and time of year, as well as the possibility of using some type of tracker with a graphic representation of the measured value - a daily graph of insolation. Matlab/Simulink software environment was used to simulate the process.

To evaluate the effectiveness of the use of a particular type of tracker, the following geographic objects were selected: Shanghai, Brno, v. Alexandrovskoe. In each of these locations the solar energy potential was evaluated. The analysis showed that all three locations have enough solar energy all year round in order to obtain with its help electrical energy to power the load of a private house.

Thus, the following data were obtained:

1.1. In the absence of a tracker and optimal azimuth and angle of inclination of the installation, the output was:

Shanghai	Brno	Alexandrovskoe
6.034 – 7.659 kW*h/ m^2	2.792 – 7.327 kW*h/ m^2	1.291 – 6.265 kW*h/ m^2

1.2. The application of the tracker by the azimuthal angle and the optimal angle of inclination of the installation gave the output in:

Shanghai	Brno	Alexandrovskoe
6.812 – 9.738 kW*h/ m^2	3.082 – 9.029 kW*h/ m^2	1.362 – 8.308 kW*h/ m^2

1.3. The application of the tracker by tilt angle and optimal azimuthal angle of installation gave a production in:

Shanghai	Brno	Alexandrovskoe
5.888 – 8.172 kW*h/ m^2	2.805 – 6.702 kW*h/ m^2	1.294 – 5.869 kW*h/ m^2

1.4. The application of the inclination and azimuth angle tracker has given a production in:

Shanghai	Brno	Alexandrovskoe
7.206 – 13.21 kW*h/ m^2	3.095 – 10.5 kW*h/ m^2	1.365 – 10.14 kW*h/ m^2

Thus, we can conclude that:

2.1 The greatest potential for solar energy has the city of Shanghai.

2.2 Depending on the location and time of year in the absence of a tracker optimal azimuthal angle of the panel is from 60 to -60 (positive angle - the direction to the South, negative - to the North) degrees.

2.3 In all geographical points, regardless of the mode of operation of the installation (stand-alone or grid), the difference from the use of trackers in relation to the system without a tracker is:

	Shanghai	Brno	Alexandrovskoe
Two-axis tracker	17.5%	8.3%	9.6%
Azimuth tracker	17%	19.5%	20%
Angle Tracker	3.5%	3.6%	7.3%

From this we can conclude that the most effective from a technical point of view is the azimuthal tracker, which gives the greatest increase in electricity generation.

The resulting models for calculating solar electricity generation were applied to power supply to a private house in the village of Alexandrovskoye with a load capacity of 9kW. The study showed that for a reliable and uninterrupted supply of electricity to the house you need the following equipment with the cost:

type of equipment	**Costs prices include VAT, rub**
Solar pannel HEVEL HJT-310 (310 Вт)	15 590,00 ₽
Fasteners for panels	27 660,00 ₽
Invertors system SILA-M 20кВт	271 200,00 ₽
Controller DOMINATOR-MPPT-200-100	87 000,00 ₽
Battery Delta GX 12-200 (200 Ah)	48 497,00 ₽
Tracker UST-VSAT	1 100 000,00 ₽
Tracker UST-AADAT	1 450 000,00 ₽

At the same time, the amount of equipment for stand-alone and network mode should be:

		Initial investment (stand-alone mode)				Initial investment (network mode)			
type of equipment	**Costs prices include VAT, RUB**	**no tracker**	**tilt tracker**	**azimuth tracker**	**tilt&azimuth tracker**	**no tracker**	**tilt tracker**	**azimuth tracker**	**tilt&azimuth tracker**
Solar pannel HEVEL HJT-310 (310 Вт)	15 590,00	159	159	144	143	58	58	53	53
Fasteners for panels	27 660,00	10	10	10	10	5	5	5	5
Invertors system SILA-M 20кВт	271 200,00	1	1	1	1	1	1	1	1
Controller DOMINATOR-MPPT-200-100	87 000,00	2	2	2	2	2	2	2	2
Battery Delta GX 12-200 (200 Ah)	48 497,00	155	155	155	155	0	0	0	0
Tracker UST-VSAT	1 100 000,00	0	2	2	0	0	1	1	0
Tracker UST-AADAT	1 450 000,00	0	0	0	2	0	0	0	1

In the paper under consideration an economic calculation was made. It is based on determining the NPV. Usually, if this indicator is positive, the project is considered profitable. However, in our case, NPV is negative, because it is based only on costs. Therefore, the main criterion was the highest NPV. Thus, the calculation showed that the most profitable to invest in the system with azimuthal tracker:

	no tracker	**tilt tracker**	**azimuth tracker**	**tilt&azimuth tracker**
stand-alone mode	-15 427 053,72 ₽	-17 895 955,16 ₽	-17 596 185,10 ₽	-18 361 759,97 ₽
network mode	-2 831 846,67 ₽	-4 066 297,39 ₽	-3 966 374,04 ₽	-4 359 153,81 ₽

It is clear that the least expensive system is without a tracker, but if we consider specifically the efficiency of one or another type of tracker, the azimuthal tracker is the most advantageous both in stand-alone and in network mode).

To summarize, it can be argued that implementing an azimuth angle tracking system in a solar installation is a technically and economically feasible solution for almost any type of terrain. The increase in power generation from its application - on average, is about 15-17%. However, to achieve maximum efficiency it is necessary to develop and start producing solar panels with high efficiency, batteries with higher capacity and low price. If these goals are achieved, the efficiency of solar trackers will increase by 10%.

Bibliography and References

1. Saganyuk V.B. Proekt novoj klassifikacii zapasov i prognoznyh resursov tverdyh poleznyh iskopaemyh. – Nedropolzovanie XXI vek, 2016. No. 1 (58) – p. 56-61.
2. Furuta K. Mitsubishi electric: energiya mirnogo atoma. – Ekonomicheskie strategii,2016. T 18. No. 8 (142) – p. 16-23.
3. Rizahanov M.A., Magomedov M.A., Kurbanova A.M. Issledovanie elektricheskih svojstv poluprovodnikovogo materiala CDS metodom adsorbcionnoj spektroskopii. – Neorganicheskie materialy,2017. T 53. No. 1 – p. 11-14.
4. Ma Wenhui, Mei Xiangyang, Wei Kuixian, Yang Bin, Dai Yongnian, Morita Kazuki. – Study on columnar crystal growth in directional solidification for solar grade silicon produced by metallurgical route. – Promising materials, 2011. №13 – p. 832-837.
5. Druzhinskij V.O. Gelioenergetika – shag v budushchee. sostoyanie i perspektivy. – Aktualnye voprosy estestvennyh i tekhnicheskih nauk,2017. – p. 26-33.
6. Seleznev A.S., Permyakova T.V. Izuchenie fotoelektricheskogo effekta. – Nauka segodnya,2015. – p. 130-132.
7. Official website NitolSolar: [Electronic resource]. Access mode: https://web.archive.org/web/20080717012635/http://www.nitolsolar.com/rutechnologies/ (Date of application 22.12.20)
8. Ribeiro D.B.S., Demetino G.G., Pepe I.M. Solar Trackers: Worldwide Map of Performances // 22nd International Congress of Mechanical Engineering. – Ribeirno Preto, Brazil, 2013. – p. 5521–5530.
9. S.G. Obuhov, I.A. Plotnikov. Vybor parametrov i analiz effektivnosti primeneniya sistem slezheniya za Solncem // Izvestiya Tomskogo politekhnicheskogo universiteta. Inzhiniring georesursov. – 2018. – T. 329, No. 10. – p. 95-106.: [Electronic resource]. Access mode: http://earchive.tpu.ru/bitstream/11683/51499/1/bulletin_tpu-2018-v329-i10-10.pdf (Date of application 22.12.20)
10. Sefa I, Mehmet D, Çolak I. Application of one-axis sun tracking system. Energy Convers Manag 2016;50:2709–18.
11. Enjavi-Arsanjani M, Hirbodi K, Yaghoubia M. Solar energy potential and performance assessment of CSP plants in different areas of Iran. Energy Procedia 2015;69:2039–48.
12. Yao Y, Hu Y, Gao S, Yang G, Du J. A multipurpose dual-axis solar tracker with two tracking strategies. Renew Energy 2014;72:88–98.
13. Masters GM. Renewable and efficient electric power systems. John Wiley & Sons; 2017.
14. Shi L, Chew MYL. A review on sustainable design of renewable energy systems. Renew Sustain Energy Rev 2015;16:192–207.
15. De Castro C, Mediavilla M. L. J. Miguel, and F. Frechoso, "global solar electric potential: a review of their technical and sustainable limits. Renew Sustain Energy Rev 2014;28:824–35.
16. Bentaher H, Kaich H, Ayadi N, Ben Hmouda M, Maalej A, Lemmer U. A simple tracking system to monitor solar PV panels. Energy Convers Manag 2014;78:872–5.

17. Skouri S, Ali ABH, Bouadila S, Salah MB, Nasrallah SB. Design and construction of sun tracking systems for solar parabolic concentrator displacement. Renew Sustain Energy Rev 2017;60:1419–29.
18. Koussa M, Cheknane A, Hadji S, Haddadi M, Noureddine S. Measured and modelled improvement in solar energy yield from flat plate photovoltaic systems utilizing different tracking systems and under a range of environmental conditions. Appl Energy 2016;88:1756–71.
19. Kassem A, and Hamad M. A microcontroller-based multi-function solar tracking system. In: Proceedings of the IEEE international systems conference. 2015. p. 13–6.
20. Koyuncu B, Balasubramanian K. A microprocessor controlled automatic suntracker. IEEE Trans Consum Electron 1991;37(4):913–7.
21. Sallaberry F, Pujol-Nadal R, Larcher M, Rittmann-Frank MH. Direct tracking error characterization on a single-axis solar tracker. Energy Convers Manag 2015;105:1281–90.
22. Li Z, Liu X, Tang R. Optical performance of vertical single-axis tracked solar panels. Renew Energy 2015;36:64–8.
23. Li Z, Liu X, Tang R. Optical performance of inclined south–north single-axis tracked solar panels. Energy 2015;35:2511–6.
24. Chang TP. Performance study on the east–west oriented single-axis tracked panel. Energy 2016;34:1530–8.
25. Chang TP. The gain of single-axis tracked panel according to extraterrestrial radiation,". Appl Energy 2016;86(7):1074–9.
26. Sun J, Wang R, Hong H, Liu Q. An optimized tracking strategy for small-scale double-axis parabolic trough collector. Appl Therm Eng 2017;112:1408–20.
27. Eke R, Sentruk A. Performance comparison of a double-axis sun tracking versus fixed PV system. Sol Energy 2016;86:2665–72.
28. Arbab H, Jazi B, Rezagholizadeh M. A computer tracking system of solar dish with two-axis degree freedoms based on picture processing of bar shadow. Renew Energy 2016;34:1114–8.
29. Song J, Yang Y, Zhu Y, Jin Z. A high precision tracking system based on a hybrid strategy designed for concentrated sunlight transmission via fibers. Renew Energy 2013;57:12–9.
30. Abu-Khader MM, Badran OO, Abdallah S. Evaluating multi-axes sun-tracking system at different modes of operation in Jordan. Renew Sustain Energy Rev 2008;12:864–73.
31. Sungur C. Multi-axes sun-tracking system with PLC control for photovoltaic panels in Turkey. Renew Energy 2015;34:1119–25.
32. Lazaroiu GC, Longo M, Roscia M, Pagano M. Comparative analysis of fixed and sun tracking low power PV systems considering energy consumption. Energy Convers Manag 2015;92:143–8.
33. Mohamad AA. Efficiency improvements of photo-voltaic panels using a Sun tracking system. Appl Energy 2004;79:345–54.
34. Ma Y, Li G, Tang R. Optical performance of vertical axis three azimuth angles tracked solar panels. Appl Energy 2011;88:1784–91.

35. Eldin SAS, Abd-Elhady MS, Kandil HA. Feasibility of solar tracking systems for PV panels in hot and cold regions. Renew Energy 2016;85:228–33.
36. Bayod-Rújula ÁA, Lorente-Lafuente AM, Cirez-Oto F. Environmental assessment of grid connected photovoltaic plants with 2-axis tracking versus fixed modules systems. Energy 2011;36:3148–58.
37. Laleman R, Albrecht J, Dewulf J. Life Cycle Analysis to estimate the environmental impact of residential photovoltaic systems in regions with a low solar irradiation. Renew Sustain Energy Rev 2011;15:267–81.
38. Tomson T. Discrete two-positional tracking of solar collectors. Renew Energy 2015;33:400–5.
39. Huang BJ, Sun FS. Feasibility study of one axis three positions tracking solar PV with low concentration ratio reflector. Energy Convers Manag 2017;48:1273–80.
40. Al-Mohamad A. Efficiency improvements of photo-voltaic panels using a Suntracking system. Appl Energy 2004;79:345–54.
41. Quesada G, Guillon L, Rousse DR, Mehrtash M, Dutil Y, Paradis P-L. Tracking strategy for photovoltaic solar systems in high latitudes. Energy Convers Manag 2015;103:147–56.
42. Seme S, Stumberger G, Vorsic J. Maximum efficiency trajectories of a two axis sun tracking system determined considering system consumption. IEEE Trans Power Electron 2011;26:1280–9.
43. Mousazadeh H, Keyhani A, Javadi A, Mobli H, Abrinia K, Sharifi A. A review of principle and sun-tracking methods for maximizing solar systems output. Renew Sustain Energy Rev 2009;13:1800–18.
44. Dakkak M, Babeli A. Design and performance study of a PV tracking system (100W − 24Vdc/220Vac). Energy Procedia 2012;19:91–5.
45. Huang BJ, Huang YC, Chen GY, Hsu PC, Li K. Improving solar PV system efficiency using one-axis 3-position Sun tracking. Energy Procedia 2013;33:280–7.
46. Ismail M, Moghavvemi M, Mahlia T. Analysis and evaluation of various aspects of solar radiation in the Palestinian territories. Energy Convers Manag 2013;73:57–68.
47. Abdallah S. The effect of using sun tracking systems on the voltage–current characteristics and power generation of flat plate PV. Energy Convers Manag 2004;45:1671–9.
48. Senpinar A, Cebeci M. Evaluation of power output for fixed and two-axis tracking PV arrays. Appl Energy 2012;92:677–85.
49. Yeh PY, Yen PC, Yen JY, Wu TT, Liu PL, Wu CL, et al. Focal point tracking system for concentration solar power collection". Renew Sustain Energy Rev 2011;15:3029–33.
50. Mathematical study of the movement of solar tracking systems based on rational models / L.M. Fernandez-Ahumada, F.J. Casares, J. Ramirez-Faz, R. Lopez-Luque // Solar Energy. – 2017. – V. 150. – P. 20–29.
51. Bahrami A., Okoye C.O., Atikol U. The effect of latitude on the performance of different solar trackers in Europe and Africa // Applied Energy. – 2016. – V. 177. – P. 896–906.
52. Tilt and azimuth angles in solar energy applications – a review / A.Z. Hafeza, A. Solimana, K.A. El-Metwallya, I.M. Ismaila // Renewable and Sustainable Energy Reviews. – 2017. – V. 77. – P. 147–168.

53. Samojlov D.V. Raschet velichiny postupleniya teploty ot solnechnoj radiacii na poverhnost zemli. – M.: Izd. MGTU im. N.E. Baumana, 2006. – 19 p.
54. Duffie J.A., Beckman W.A. Solar Engineering of Thermal Processes. 4th ed. – Hoboken, New Jersey: John Wiley & Sons, Inc., 2013. – 910 p.
55. Matveev L.T. Kurs obshchej meteorologii. Fizika atmosfery. L.: Gidrometeoizdat,1984. – 752 p.
56. The website Weather and Climate: [Electronic resource]. Access mode: http://www.pogodaiklimat.ru/weather.php?id=29430&bday=15&fday=15&amonth=7&ayear=2017&bot=2 (Date of application 16.02.21)
57. The website NASA Surface meteorology and Solar Energy: [Electronic resource]. Access mode: https://eosweb.larc.nasa.gov/cgi (Date of application 22.02.21).
58. The website United Smart Technologies: [Electronic resource]. Access mode: http://ust.su/solar/catalog/trackers/3120/ (Date of application 01.11.21).
59. Budzko I.A., Levin M.S. Elektrosnabzhenie selskohozyajstvennyh predpriyatij i naselennyh punktov. 2-e izd., pererab. Dop. – M.:Agropromizdat, 205. – 320 p., table 3.3
60. The website Tekhnolajn: [Electronic resource]. Access mode: https://e-solarpower.ru/solar/solar-panels/mono-panel/solnechnaya-batareya-silasolar-350vt-perc-5bb/ (Date of application 01.11.21).
61. The website Delta: [Electronic resource]. Access mode: https://www.delta-batt.com/catalog/section.php?SECTION_ID=180 (Date of application 01.11.21).
62. The website Tekhnolajn: [Electronic resource]. Access mode: https://e-solarpower.ru/solar/inverter/hybrid-inv/sistema-invertorov-sila-m-20kw/ (Date of application 01.11.21).
63. Resolution No. 334 of the Government of the Russian Federation of April 21, 2009 "On Amending Certain Acts of the Government of the Russian Federation Regarding the Improvement of the Procedure for Technological Connection of Consumers to Power Grids"
64. Manufacturer's website on the site Alibaba: [Electronic resource]. Access mode: https://russian.alibaba.com/product-detail/dual-axis-solar-tracker-control-and-drive-kit-dual-axis-sun-pv-tracking-driver-combo-kit-1600197181906.html?spm=a2700.galleryofferlist.topad_classic.d_image.52154a61PIbM9A (Date of application 05.12.21).
65. Manufacturer's website on the site Alibaba: [Electronic resource]. Access mode: https://russian.alibaba.com/product-detail/china-slew-drive-se25-with-hydraulic-motor-for-solar-tracker-system-use-62386390102.html?spm=a2700.galleryofferlist.normal_offer.d_image.52154a61PIbM9A&s=p (Date of application 05.12.21).
66. Lukutin B.V. Renewable power sources: textbook. - Tomsk: TPU Publishing House, 2008. - 187 c.
67. Brealey, R.A., Myers, S.C.: Principles of Corporate Finance. McGraw-Hill. 2002
68. Russian Government Bond Zero Coupon Yield Curve, [Online]. Available: https://www.cbr.ru/eng/hd_base/zcyc_params/. [Accessed 2.04.2022].

69. Stephen, A.R., Randolph W.W., Bradford D.: JordanFundamentals of Corporate Finance Standard Edition. McGraw-Hill. 2005